UC-80

ETR POWER–VARIATION ANALYSIS

E. E. Burdick
J. L. Liebenthal

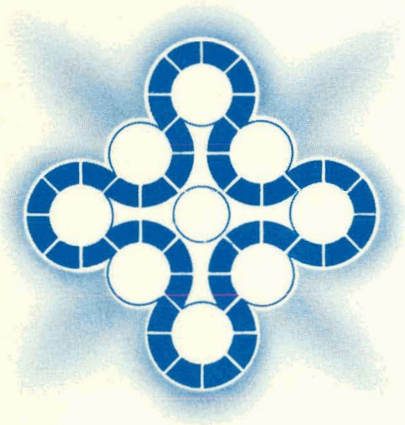

Aerojet Nuclear Company

NATIONAL REACTOR TESTING STATION

Idaho Falls, Idaho — 83401

Date Published — August 1972

PREPARED FOR THE
U. S. ATOMIC ENERGY COMMISSION
IDAHO OPERATIONS OFFICE UNDER CONTRACT AT(10-1)-1375

DISCLAIMER

Printed in the United States of America
Available from
National Technical Information Service
U. S. Department of Commerce
5285 Port Royal Road
Springfield, Virginia 22151
Price: Printed Copy $3.00; Microfiche $0.95

ANCR-1085

Reactor Technology
TID-4500

ETR POWER-VARIATION ANALYSIS

E. E. BURDICK J. L. LIEBENTHAL

CONTRIBUTORS

R. G. AMBROSEK
S. A. ATKINSON
A. L. BOWMAN
R. L. COPYAK
R. W. KELLER
S. R. GOSSMANN
M. L. GRIEBENOW
D. H. SCHOONEN

AEROJET NUCLEAR COMPANY

Date Published -- August 1972

PREPARED FOR THE U. S. ATOMIC ENERGY COMMISSION
IDAHO OPERATIONS OFFICE
UNDER CONTRACT NO. AT(10-1)-1375

ABSTRACT

Between June and December 1971, small (nominally ±0.5% amplitude), intermittent power variations of unknown origin were witnessed at the Engineering Test Reactor. This report is the result of the investigative program carried out by Aerojet Nuclear Company to determine the cause of the variations. Included in the report are diagnostics, inspections, and analyses.

C O N T E N T S

F I G U R E S

T A B L E S

1. INTRODUCTION AND SUMMARY

During the Engineering Test Reactor (ETR) Cycle 112B startup on June 8, 1971, it was observed that the differential power level recording on all neutron flux monitors indicated a small but definite power variation (PV). The amplitude, nominally one percent peak-to-peak of total power, was no larger than that experienced on several other occasions. However, the variation on this occasion had a more definite frequency than had been experienced before. The period of the variation was nominally three seconds.

An analysis of the recordings indicated that the reactivity driving force was nominally one cent and that the amplitude and frequency were independent of the power level. Moreover, a review of in-core neutron flux and temperature transducers indicated no anomalous power distribution. Also, a failure-mode and consequence analysis showed that the power variations were not an indication of risks not already considered. Therefore, operation continued under close surveillance while an investigative program was planned and conducted.

This report is a summary of the investigative program and its findings. The investigative program consisted of (a) a diagnostic program (described in Section 3. and occurring during the period of June to December 1971) consisting of varying system parameters which could conceivably have an effect on power variation, (b) core component inspections (Section 4.) during shutdown for evidence of moving components, restricted coolant passages, and gas leaks, and (c) analyses of abnormal conditions and unusual experiment designs (Section 5) to determine if they were a possible source of the PV.

Many measurements were made and many parameters varied in an effort to identify the source of the power variation. Measurements were made to confirm that the apparent PV was real and not a false indication resulting from electrical noise. Flow was varied in the primary, secondary, and loop coolant systems to test for flow-induced mechanical movement and thermally-induced effects. Primary and loop system pressures and temperatures were varied and reactor integral power was changed to test for thermally-induced effects. Pressures were varied on experiments containing in-tank gas volumes to test for possible gas leaks into the core. Finally, the power distribution was perturbed into many different shapes in an attempt to identify the location of the driving force. This was accomplished by changing the control-rod position configuration.

The above mentioned tests and analyses indicated the PV driving force was not flow-induced mechanical movement, open channel boiling, or gas leaks. However, changes in reactor integral power and power distributions did indicate the possibility of a thermally-driven source. Moreover, the power distribution changes indicated the PV source to be

in the vicinity of Rod 14. These results led to the inspection for flow restrictions in core components near Rod 14[a], and the removal of experiments in core positions J8 and J10.

Following the cleaning of all removable 4X pieces and the removal of the two experiments, the reactor returned to power on December 8, 1971, with no power variation. The characteristics of the power level trace have varied little since that startup.

Because the power variations stopped after cleaning the core and the removal of the two experiments (ACRH in J10 and ORNL in J8), it is concluded that some condition associated with these two experiments and/or experimental position coolant channel flow blockage was the cause of the PV. "Cause Analysis" (Section 5) failed to positively identify the exact condition that caused the PV. As summarized below, the analyses did show that a special set of conditions was necessary to produce the variations.

(1) The low-heat-output (<2.5 W/g gamma heat) aluminum filler pieces cannot cause voiding because the heat can be removed through a stagnant water annuli without boiling. Aluminum fillers with greater than 2.5 W/g could boil, but at a frequency of about 4 Hz. An even higher-heat-output stainless steel filler would cause boiling in stagnant water, but at a frequency of about 30 Hz. Because the observed frequencies are greater than 0.3 Hz, some special flow blockage condition would be required to produce the right frequency. Such a condition cannot be ruled out.

(2) One of the experiments removed, ACRH (J10) showed apparent "temper colors" indicating temperatures in the 600°F range had been experienced on stainless solid spacers in the capsule train. This proved that voiding had occurred for at least a short period of time. However, metallurgical examinations of the stainless steel spacers did not confirm that such temperatures had existed for the length of time oscillations were observed. Nevertheless, boiling in ACRH capsules cannot be completely ruled out. Again, unique conditions would be required to produce boiling. The capsule train in its "designed" original condition was reinserted without a resultant power variation.

(3) The ORNL (J8) capsules were shown by analysis to have a thermally-induced mechanism whereby power variations of the proper period could be produced. Reinsertion of the ORNL experiment did not cause a reoccurrence of the oscillations. Possible differences in gamma heat gradients and holder (X basket) dimensions between the original and reinserted conditions leave the possibility that the ORNL experiments could have caused the PV.

---

[a]Because some 4X piece flow restriction was found near Rod 14, all removable 4X pieces within the core were inspected. Flow restriction was also found in other areas of the core.

Throughout the course of the PV study, efforts were made to show that the power variation was not an indication of an incipient instability. These efforts included a rod-drop experiment and stability analysis. Results of this program[1] indicate a stable system with a gain margin much greater than 10.

2. HISTORY AND CHARACTERISTICS

Since the initial startup, differential power level recordings have been taken at various power levels during each startup to monitor for conditions which cause power variations. These recordings were made with Brush recorders which have the capability of bucking out the dc component and amplifying the ac component of the signal.

A review of available recordings (not sent to storage) indicates that on several occasions since 1963 and before June 1971, the ETR experienced small power variations[a]. These variations were less than 1.4% in amplitude, were aperiodic except in one case, and existed for only one or two consecutive startups. This is illustrated in Figures 2-1, 2-2, and 2-3 where selected recordings for the period of 1963 through 1971 show the appearance and disappearance of power variations. As shown, the amplitudes range from near zero to 1.4%. The period of variation is discrete only for the 4/9/69, 120 MW recording. It will be noted that this discrete period disappeared when full power was reached. In another example (12/14/68) it will be noted an apparent power variation at 120 MW changed significantly and was almost nonexistent at 175 MW. The causes of the power variations prior to June 1971 were never identified nor were any deleterious effects detected.

Although the variation detected on June 8, 1971, (Cycle 112B) had a relatively consistent amplitude of 1 - 1.6% and a period of 3 - 5 seconds for three days, it evolved into a variation with widely varying characteristics. Its character changed without any correlative change in any reactor parameter. Variations in amplitude and period are shown in Figure 2-4, and signal shapes are shown in Figures 2-5, 2-6, and 2-7. As shown, amplitude varied from near zero to 2.6%, and the period varied from 1 to 44 seconds. Variations with periods greater than 20 seconds were proven to be caused by temperature variations in the M7 loop, caused by a minor problem in the controller. There was one brief period of time at a power below 100 MW that the period was as short as 0.3 seconds. Examples of changes in characteristics are as follows: (a) variations would cease for periods of time varying from 10 sec to 113 hrs, (b) there were variations during some startups that would cease or diminish in amplitude shortly after reaching full power, while during other startups there would be no variations initially, but later a variation would develop, (c) the rate of change varied from quite rapid to gradual, and (d) on one occasion (11/23/71) a larger-amplitude and shorter-period variation resulted following a power reduction to 140 MW. Prior to the reduction the reactor had operated for 33 hours with a variation of 0.5 to 0.7% amplitude, with a three-second period. When the power was decreased to 140 MW the amplitude increased to 1.3% with a period of 1.1 sec. After returning to full power the variation gradually changed to one with a 2.1 to 2.6% amplitude and a period of 3 to 4 seconds. Three sample recordings are shown in Figure 2-7.

---

[a]There have been three ETR events[2] which produced power variations for which there are no differential power level recordings available: (a) sight-glass blockage of several fuel elements[3], (b) adhesive tape blockage of one fuel element[4,5], and (c) vibration of the flow tube within an in-pile loop[6].

The change in conditions discussed under (d) above led to a shutdown on November 23, followed by an intensive diagnostic program discussed in the next sections. Following this program and a shutdown during which the flow passages of several experiment holder (4X) pieces were cleared and two suspicious experiments were removed, the reactor returned to power on December 8, 1971, with no power variation, as shown in Figure 2-7.

Recordings taken between December 1971 and July 1972 show that most of the power signal recordings have very low noise components (<±0.1 percent) as represented by recordings for 1/27, 3/13, 4/26, 6/21, and 7/15/72. (Figure 2-8). This condition also applies to those recordings (3/13 and 7/15) taken following the reinsertion of the two suspicious experiments (see Sections 5.2 and 5.3). Two conditions were found to produce noisier-than-usual recordings. On one occasion temperature variations in the M7 loop were observed to be coincident with the noisy (± 0.1% amp. and ∿ 0.7 sec period) power recording of 6/21 (Figure 2-8). Fine tuning the loop controls caused the temperature and power variations to stop, as indicated in the other 6/21 recording. The other condition which caused the power signal noise component to increase was associated with control rod positions. During both cycles in which rod bank 6-2-16 was withdrawn the power signals became noisier. As shown in the representative paired recordings of 1/27-2/13 and 4/26-5/8 the noise increased from <±0.1 percent up to ±0.4 percent, but with no unique period of variation. No similar correlation could be found with the data which preceded January 1972. Evidence of a correlation since that date probably results from the combination of the existence of less noisy signals and having more data. If the correlation is real it is probably caused by the combined effect of more withdrawn rods in the core and reactivity statistical weight distribution changes. Because these increases in noise levels are small and have no unique frequency no diagnostic effort is planned.

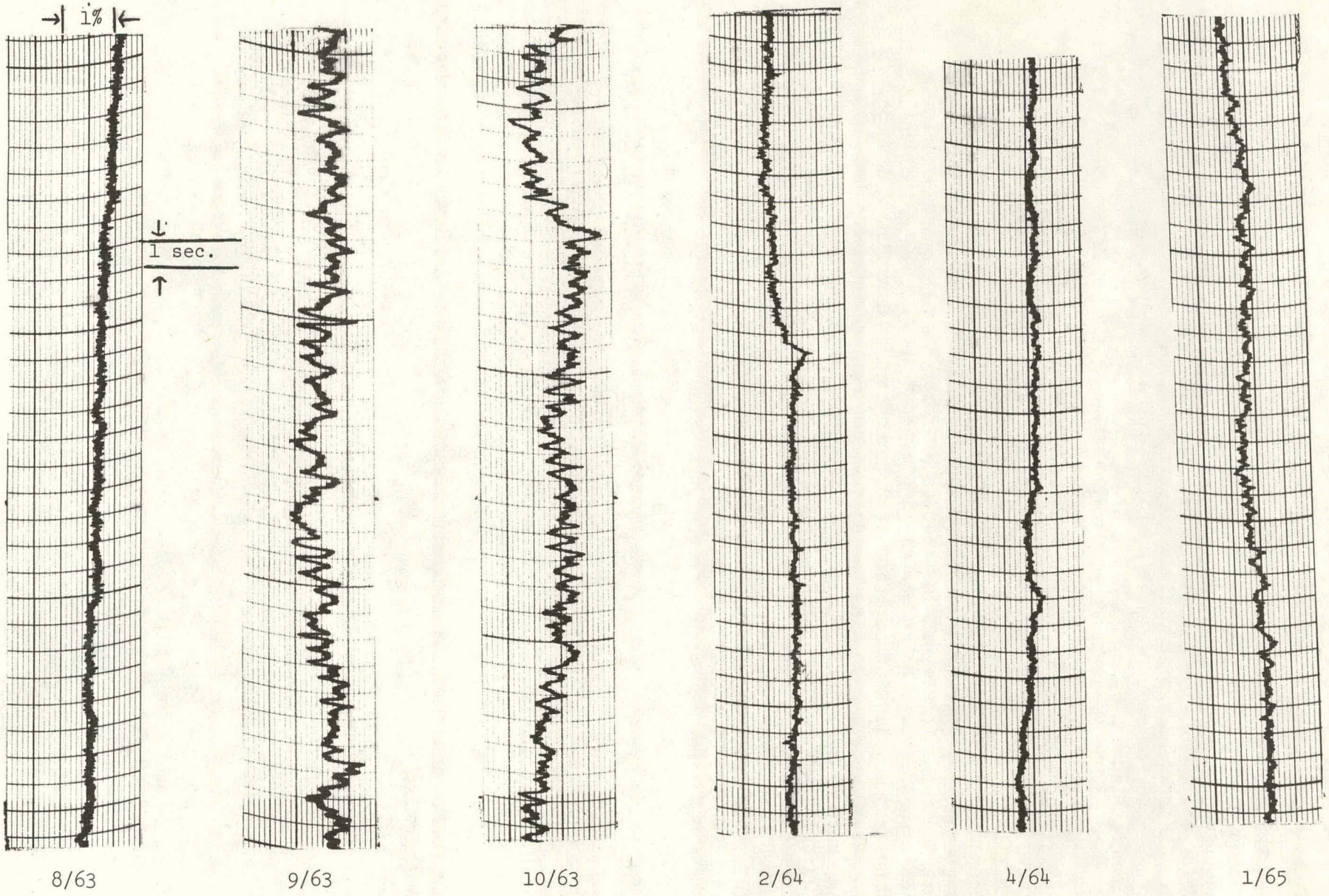

Figure 2-1. Samples of ETR power level recordings for the period of August 1963 through January 1965. All recordings were made at or within 5% of full power (175 MW).

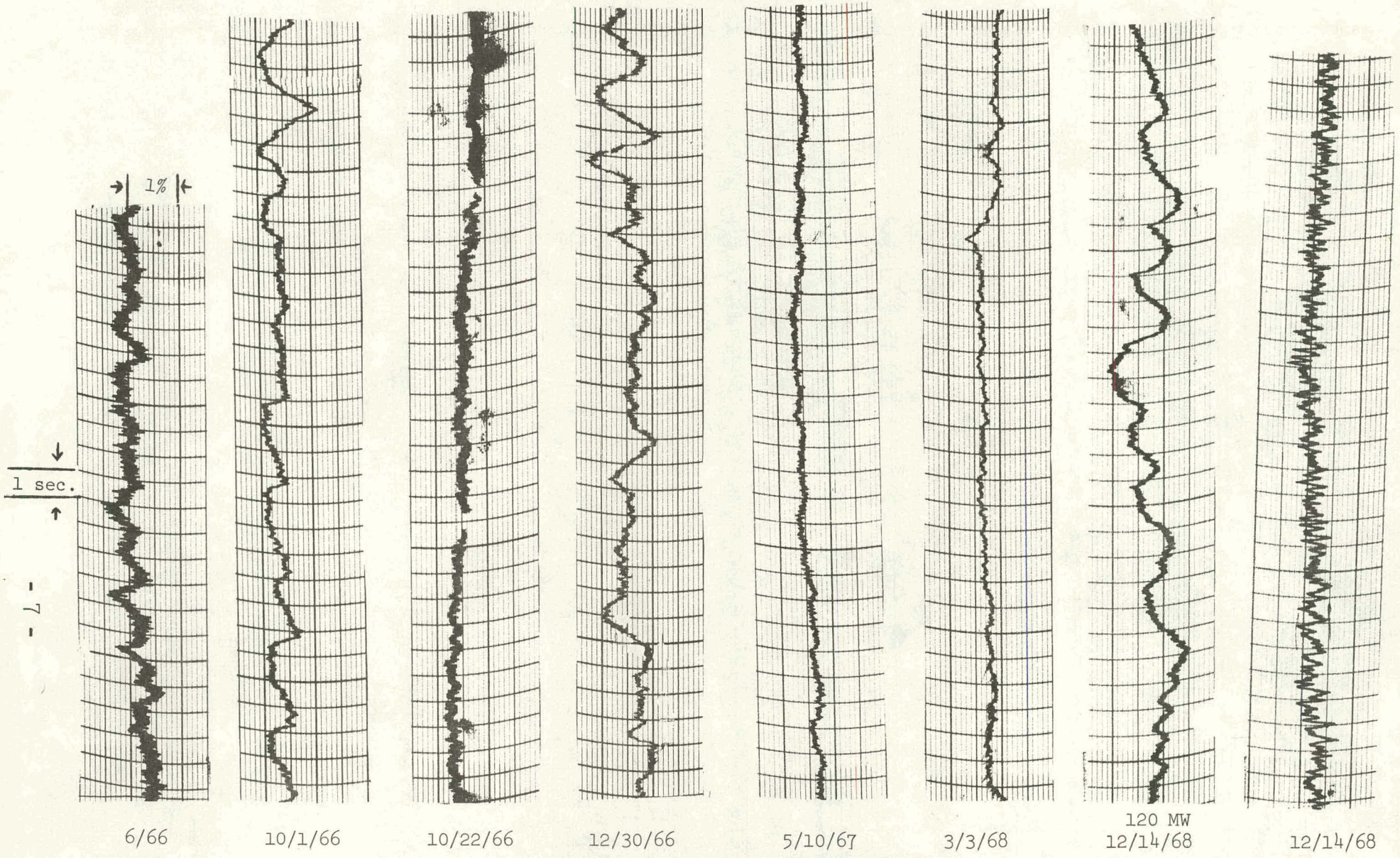

Figure 2-2. Samples of ETR power level recordings for the period of June 1966 through December 1968. Except as noted all recordings were made at or within 5% of full power (175 MW).

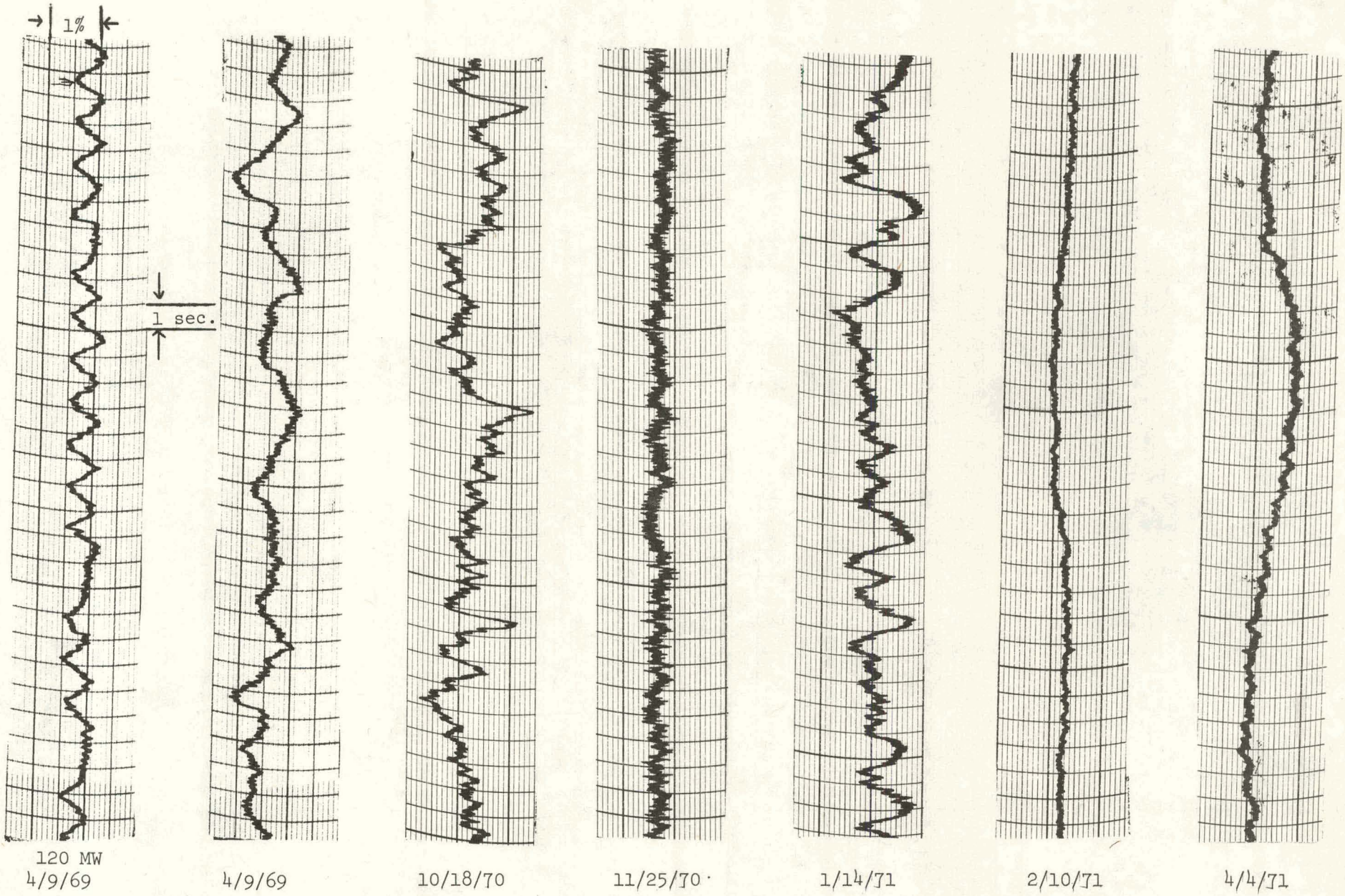

Figure 2-3. Samples of ETR power level recordings for the period of April 1969 through April 1971. Except as noted all recordings were made at or within 5% of full power (175 MW).

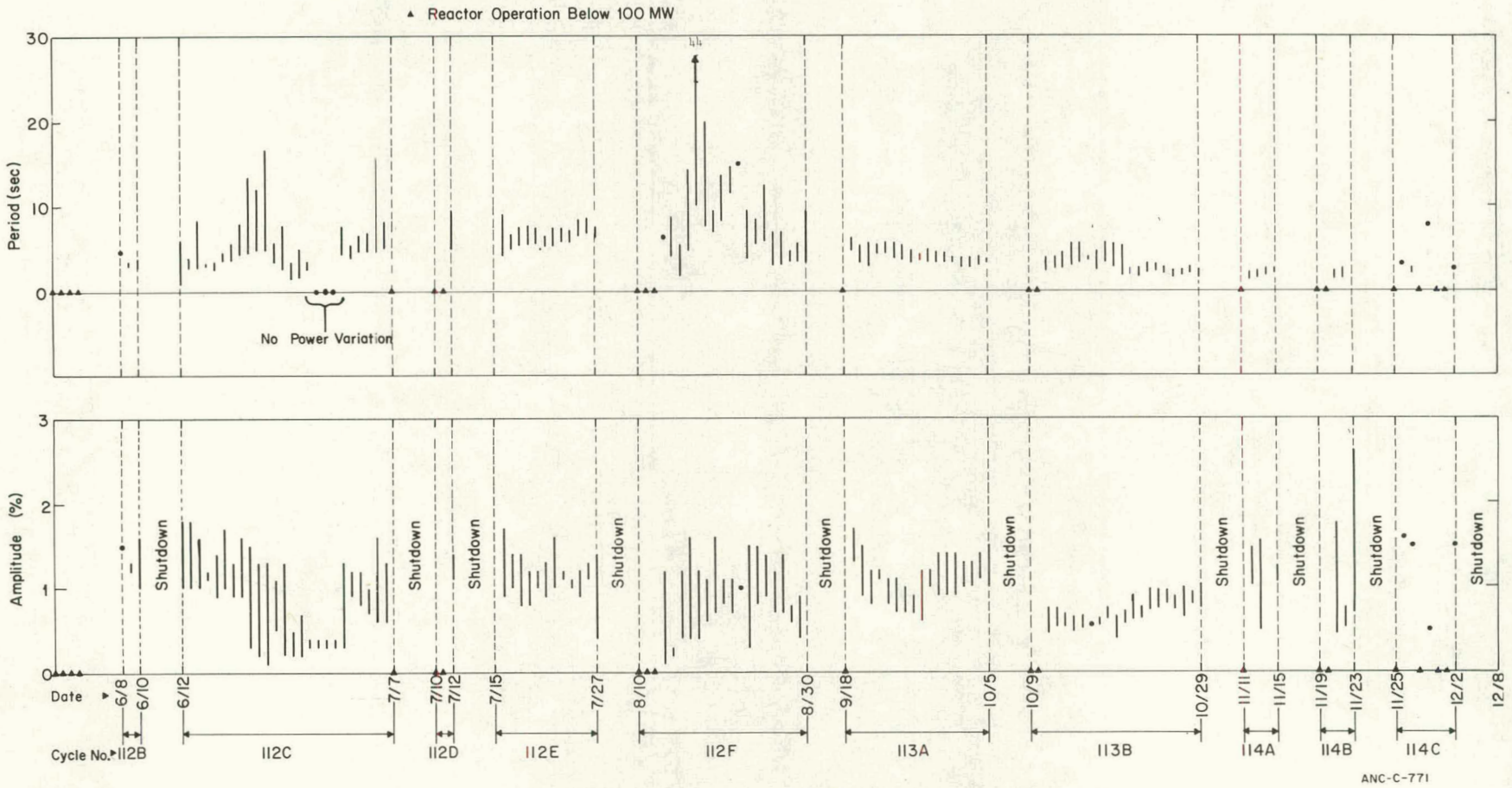

Figure 2-4. Daily range of the period and amplitude of ETR power variations during the period of June to December 1971.

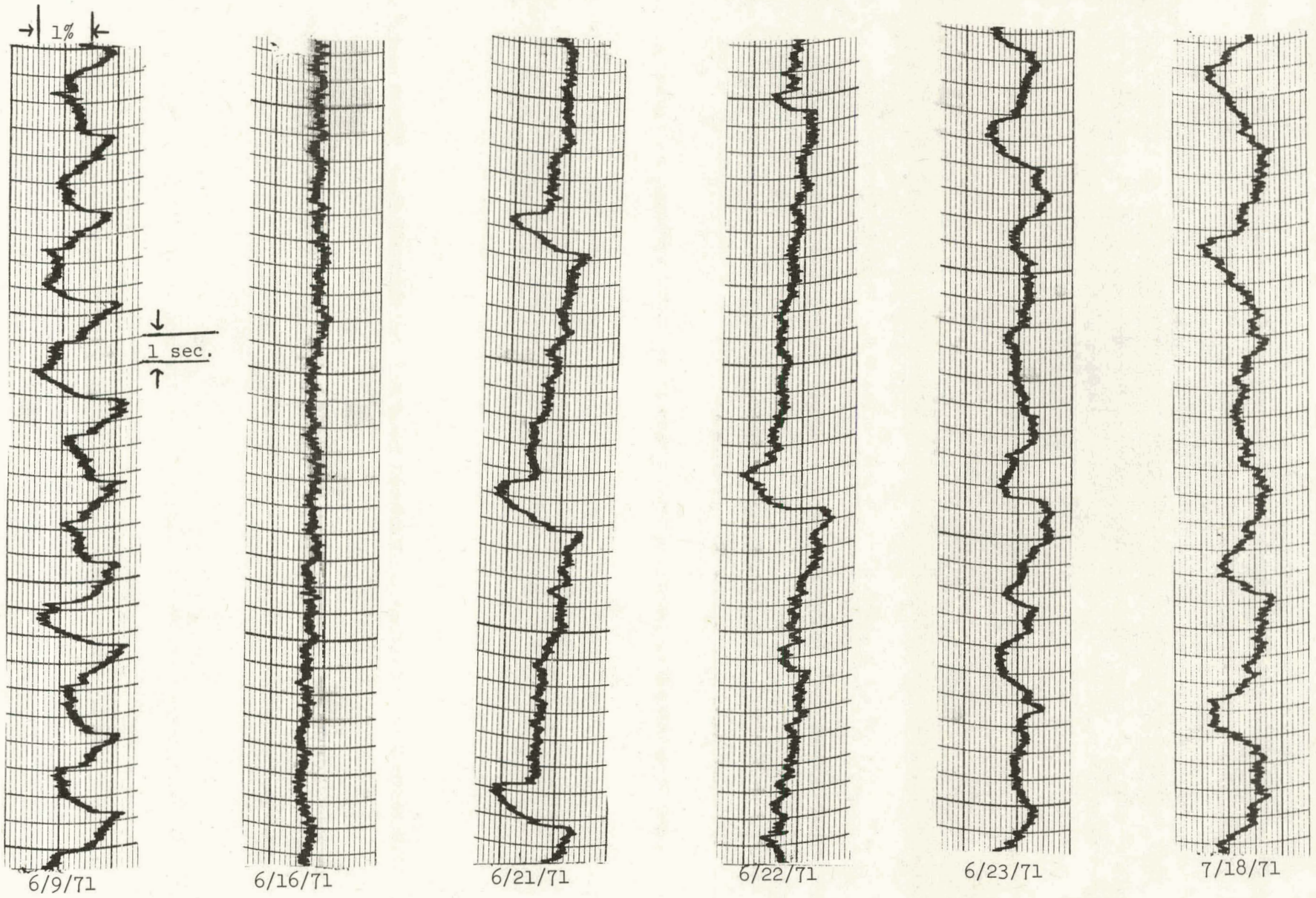

Figure 2-5. Samples of ETR power level recordings for the period of June 1971 through July 1971. All recordings were made at or within 5% of full power (175 MW).

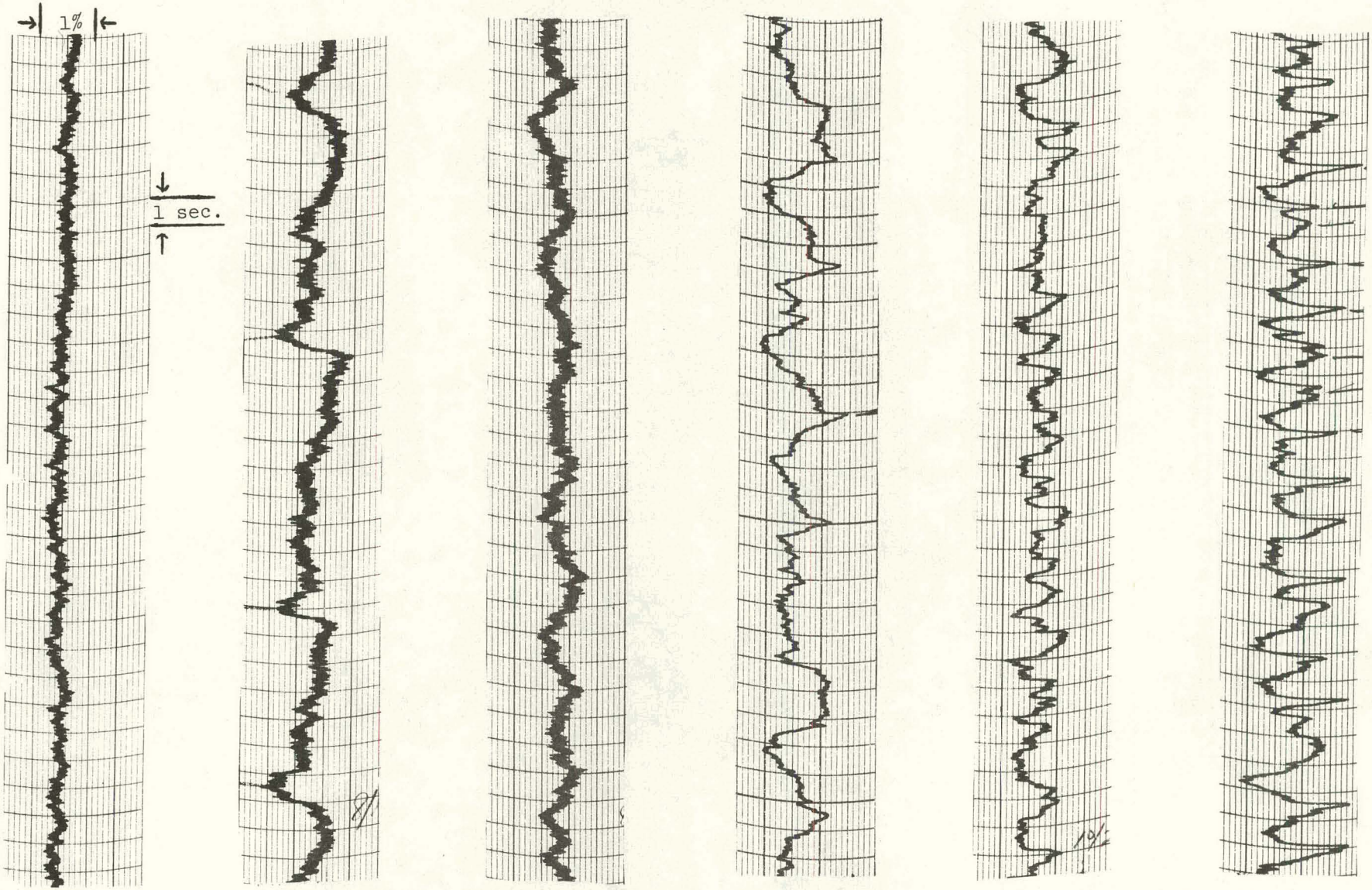

Figure 2-6. Samples of ETR power level recordings for the period of August 1971 through November 12, 1971. All recordings were made at or within 5% of full power (175 MW).

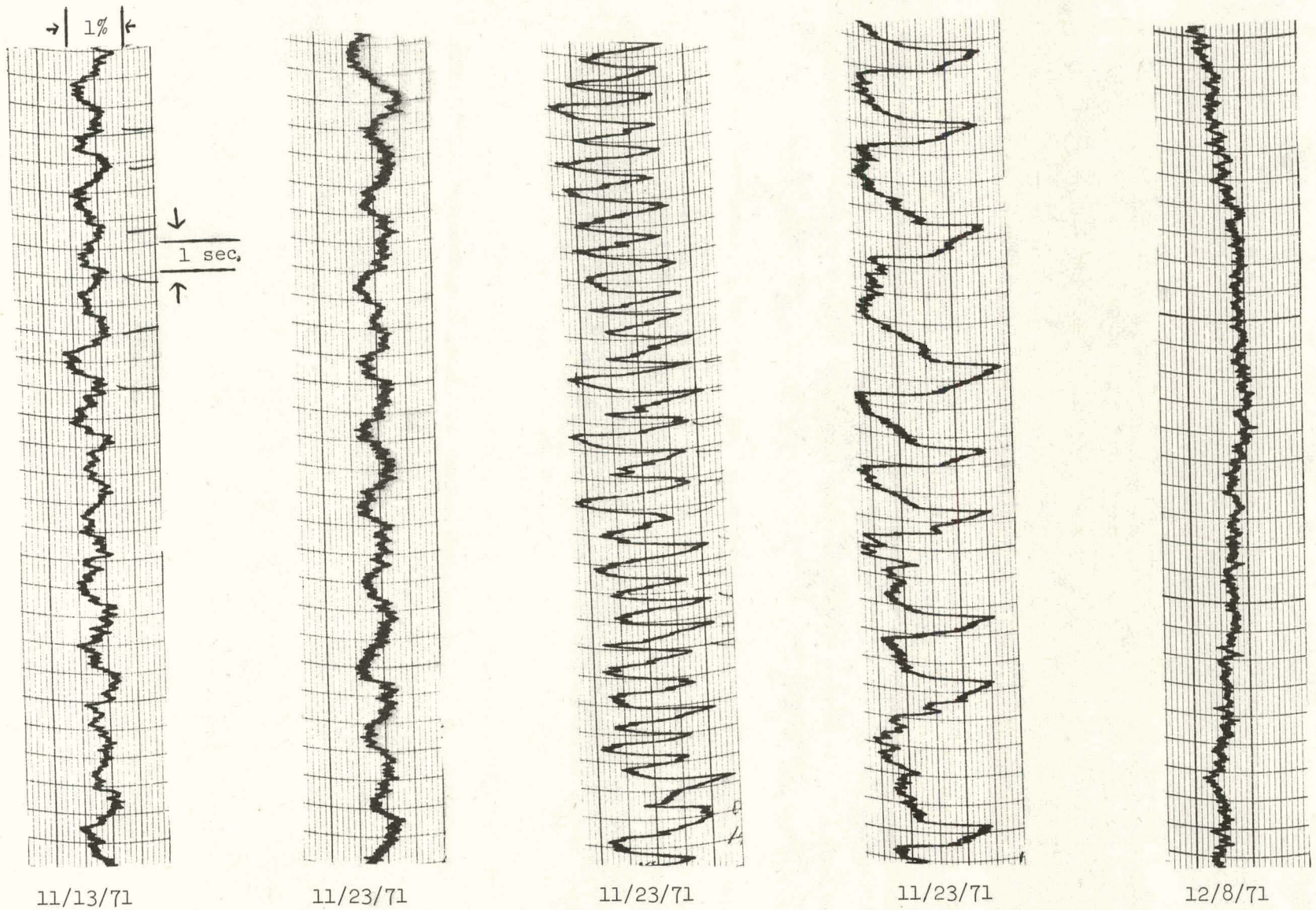

Figure 2-7. Samples of ETR power level recordings for the period of November 13, 1971, through December 8, 1971. All recordings were made at or within 5% of full power (175 MW).

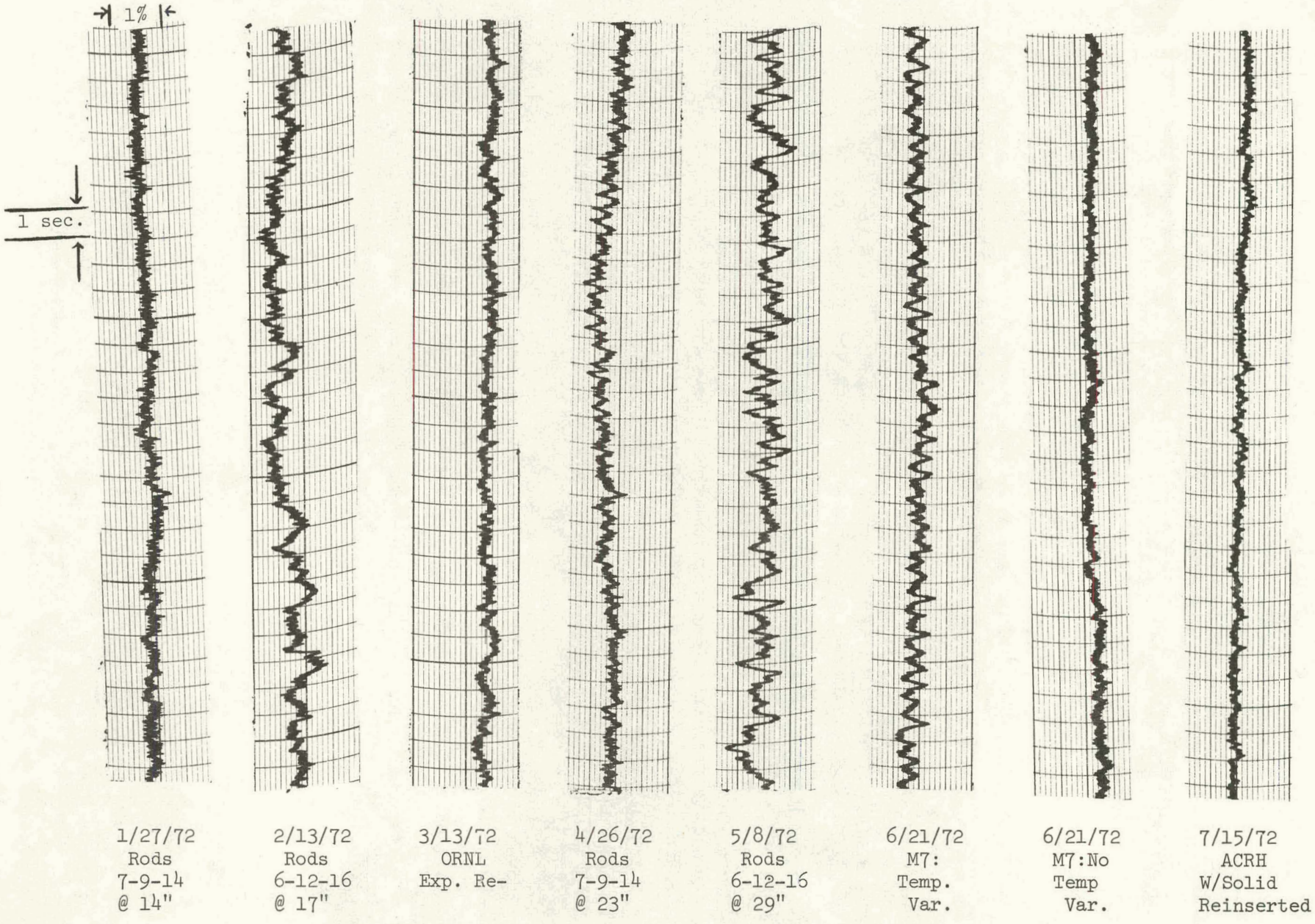

Figure 2-8. Samples of ETR power level recordings for the period of January 1972 through July 1972. All recordings were made at or within 5% of full power (175 MW).

3. DIAGNOSTIC PROGRAM

3.1 Electrical Noise

Early in the diagnostic program recordings were made to eliminate electrical noise as the source of the apparent variation. Recordings taken under several different conditions showed that the ETR power variations were real and not the result of the 117 Vac power system or related ground loops. These were several recordings of a constant current source, several reactor flux signals, and a battery-powered reactivity meter[7,8]. The reactor flux signals were obtained from various instrument-conditioned signals using three ion chambers and two fission chambers as detectors of the power variation. These chambers are located permanently in the reactor instrument thimbles.

The intent of these recordings was to define the characteristics and to pinpoint by elimination the source of the apparent reactor power variations. The approach followed was first to establish good baseline recordings. This baseline was used for description of the indicated power variation and for comparison to other recordings. Second, recordings were made using different measuring instruments on different 117 Vac power systems with different or floating grounds. Third, recordings were made using a different type of radiation detector as the signal source in several applications. Finally, recordings were made with a battery powered system. In addition, in each instrument configuration a recording was made using a current source in place of the chamber signal. The devices involved were standard ion and fission chambers, microammeters, reactor instruments, a current source, a reactivity meter, a two-channel Brush strip-chart recorder, a magnetic tape recorder, and a 117 Vac power stabilizer used under the various conditions shown in Table 3.1-I and Figure 3.1-1. A summary of the test results follows.

Recordings No. 1, 2, 3, and 4, Table 3.1-I, are the baseline recordings from permanently installed plant instruments. These recordings established that the signal variations existed on each level channel of the Plant Protection System in its normal configuration (shown in Recordings No. 1 and 2, Figure 3.1-1). The signal from these three ion chambers showed that the power variation could be observed in the north, southeast, and southwest regions of the reactor. Also, a recording made when a current source was used in place of the ion chambers established that the indicated power variation was not generated in the instrument channels.

Recordings No. 5 and No. 6[a] established that the power variation could be observed on a different type of measuring instrument (microammeter) and that the level preamplifier could not be the source of the variation.

Recordings No. 7 and No. 8[a] established that the power variation was independent not only of the level preamplifier but also of the 117 Vac instrument power system.

Recordings No. 9 and No. 10[a] established that the power variation present when monitored on the level preamplifier remained independent of the 117 Vac instrument power system.

---

[a]A current source was used in place of the chamber signal for these measurements in order to separate the ion chambers and the measuring devices as the source of the apparent power variation.

From Recordings No. 11 and 12 power spectral density analysis determined the frequency characteristics of the variations and established that the power variation could be observed on fission chambers as well as ion chambers.

Recording No. 13 established a measured reactivity magnitude for the variation and utilized another type measuring device.

Recording No. 14 established that the power variation could be observed on an electrically isolated system.

Recordings No. 7, 8, 9, and 10 also indicated that plant grounds were not the source of the reactor power variations. However, Recording No. 14 was made specifically to rule out plant grounding. Moreover, Recordings No. 11, 12, and 13 indicated grounding problems were unlikely since those recordings were made of the output of a single amplifier, carefully grounded, which used a single point ground and a very short, controlled-ground loop.

Noise pickup (as in an antenna) in the chamber output cable was ruled out because the variation consistently appeared in all signals regardless of location, type of chamber, or cable installation. The results of several independent recordings were the same--the output signals of the ion and fission chambers indicated real reactor power variations, and all other sources associated with the instruments did not contribute.

TABLE 3.1-I

RECORDING CONDITIONS

Recording Number	Signal Source	Signal Measuring Instrument and Monitoring Point	External Connections	Recording Device	AC Power
1	CIC and Level Nos. 1, 2, & 3 Preamp.	Input of Sigma Amplifier	Normal	Brush	Instrument Bus MG-3
2	Current Source at Level No. 2 Preamp. Input	Input of Sigma Amplifier	Normal	Brush	Instrument Bus MG-3
3	CIC Level No. 2	Output of Level No. 2 Preamp.	Output to Sigma Amp. Disconnected	Brush	Instrument Bus MG-3
4	Current Source	Output of Level No. 2 Preamp.	Output to Sigma Amp. Disconnected	Brush	Instrument Bus MG-3
5	No. 2 Level CIC Battery Powered	Output of Keithley Model 410		Brush	Instrument Bus MG-3
6	Current Source	Output of Keithley Model 410		Brush	Instrument Bus MB-3
7	No. 2 Level CIC Battery Powered	Output of Keithley Model 410		Brush	Output of ac Stabilizer on Com. Power
8	Current Source	Output of Keithley Model 410		Brush	Output of ac Stabilizer on Com. Power
9	No. 2 Level CIC Battery Powered	Output of Level Preamp.	Output to Sigma Amp. Disconnected	Brush	Output of ac Stabilizer on Com. Power
10	Current Source	Output of Level No. 2 Preamp.	Output to Sigma Amp. Disconnected	Brush	Output of ac Stabilizer on Com. Power
11	Fission Chamber in B-1	Current Sensitive Amplifier		Mag. Tape	Com. Power
12	Fission Chamber in B-5	Current Sensitive Amplifier		Mag. Tape	Com. Power
13	Fission Chamber in B-5	Output of Reactivity Meter		Brush	Com. Power
14	Fission Chamber in B-5	Output of Reactivity Meter		Brush	dc Power

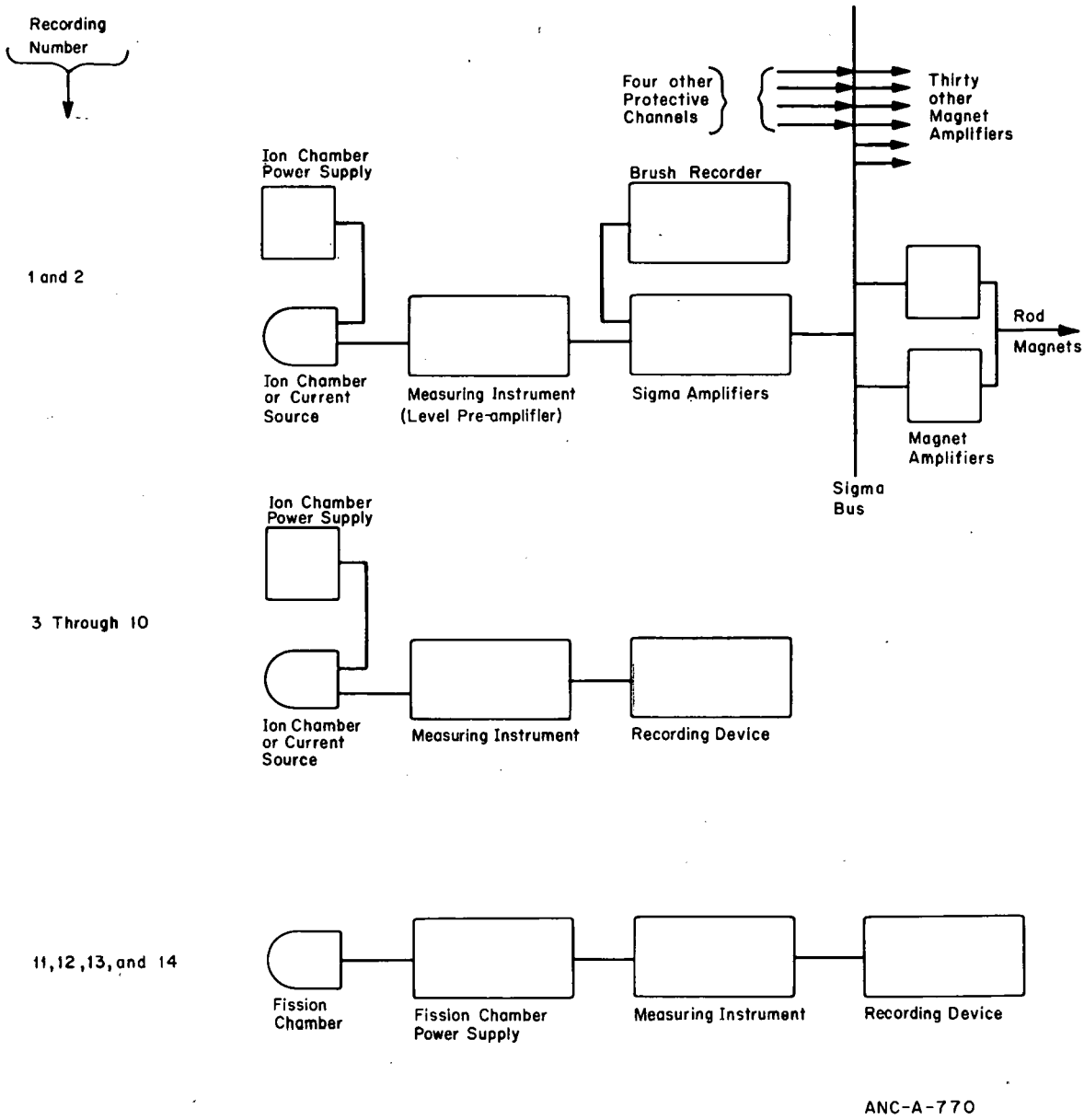

Figure 3.1-1. Instrumentation used in testing for electrical noise.

3.2 Power Distribution Effects

The amplitude of a power variation caused by localized mechanical movement, boiling, or gas-induced voids within the core is dependent upon the core power distribution, whether or not the driving force is within or outside the experiment loops. The amplitude is affected because the reactivity statistical weight is nearly proportional to the square of the local neutron flux. The flux distribution can also affect a boiling driving force because the local power density has a direct effect on the steam void production rate. Considering the foregoing, it is obvious that changes in the power distribution could be used as a diagnostic tool for identifying the general location of the driving force. In order to take advantage of this phenomenon, the effect of different control rod position configurations on the power variation was studied.

ETR control rods are composed of poison pieces and fueled followers (see Figure 3.2-1), arranged within the core as shown in Figure 3.2-3. To attain criticality, to compensate for fission product poisoning, and to compensate for fuel burnup, the control rods are withdrawn in the following sequence:

(a)	1, 2, 3, 4	individually
(b)	8, 10, 13	individually
(c)	5, 11, 15	banked within one inch
(d)	7, 9, 14	banked within one inch
(e)	6, 12, 16	banked within one inch

Throughout the period of these power variations, initial criticality was attained high on the 5-11-15 bank, for normal operation. Fission product poisoning caused the rods to move on to the 7-9-14 bank usually before full power was reached. The 6-12-16 bank is withdrawn only to override xenon following scrams and to compensate for burnup after ~5000 MWd.

Axial and radial power distribution changes result from the normal rod movements described above. Normal rod movement occurs slowly and has small effects on horizontal power distribution because the three rods tend to counteract one another. The normal power distribution can be significantly skewed by moving rods out of the normal rod program. In an attempt to identify the location of the driving force as closely as possible, many different rod position configurations were produced, hereafter referred to as rod effects tests (RET). These configurations were produced by moving (withdrawing and inserting) rods out of their normal configuration in the following general ways: (a) a single rod compensated by the controlling rod bank, and (b) a single rod compensated by another single, nearby rod (paired rods). (These rods had to be selected in pairs of one withdrawn and one inserted rod). Method (a) caused gross flux shifts across the core, therefore could be expected to give only a gross indication of the location. Method (b) caused more localized flux perturbations; therefore was expected to give a more precise indication of the location. Because these rod manipulations do cause significant power,

and thus heat flux distribution changes, the RET could not be performed above 80 MW. This produced complications. When the reactor power was above 80 MW a programmed power reduction had to be used to avoid losing the reactor to xenon. Also, because of the capricious nature of the power variation, it was not always present when 80 MW was reached, either during startup or after power reductions. These tests were, therefore, not conducted at will. RETs were performed or attempted on six different occasions: (a) June 19-20 (Cycle 112C), (b) June 22 (Cycle 112C), (c) July 7 (Cycle 112C), (d) July 11 (Cycle 112D), (e) Oct 10 (Cycle 113B), and (f) Nov. 26 and Dec 2 (Cycle 114C). These tests were interspersed with other diagnostic tests described in other parts of this report.

Moving rods during these RETs also allowed a direct test for the effect of mechanical movement in the control rods. The rod bearings are located in the poison piece (Figure 3.2-1) and in the shock section below the fuel section. Moving the rod changes the positions of the rod components relative to the core. If a faulty bearing, fuel plate, etc., were allowing lateral movement of a rod, changing its position would change the rod displacement amplitude within the core and thus change the resulting reactivity amplitude.

Power variation dependency on normal rod movements was studied throughout the period of June through November. At no time could a correlation be found which gave a strong indication of the location of the driving force. A composite summary of all the data collected is shown in Figure 3.2-2. As shown, correlations are weak compared to the size of the error bars. These correlations are judged especially weak in view of the fact the power variations stopped for varying periods of time when there was no known change in reactor conditions.

The RET performed during the period of June through October (along with the mechanical inspection of all rods) served to absolve the rod components of lateral motion and gave indications that the driving force was in the northeast region of the core. A summary of the power variation characteristics with different rod configurations is presented in Table 3.2-I.

As shown the only movements that caused a significant effect on the amplitude and period were inserting Rod 2 and withdrawing Rods 12 and 16. These three rod movements have the common effect of causing the neutron flux to decrease in the northeast region of the core. No significance could be attached to the changes in period associated with Rods 4, 6, and 14. It was these data plus the fact the M7 test (located in the NE region) was the only loop test not changed out since June 71, which led to removing the M7[a] test during the Cycle 114C shutdown.

The RETs performed during the period of November 26 - December 2 gave strong indications the driving force was located in the vicinity of Rod 14. The results of two different series of measurements are shown in Figure 3.2-3. The first series consisted of single rod movements

---

[a] The L12 test was removed at the same time because the two loops use common out-of-pile equipment which requires that both loops be either loaded or unloaded.

TABLE 3.2-I

SUMMARY OF POWER VARIATION CHARACTERISTICS FOR THE MOVEMENT OF A SINGLE ROD COMPENSATED BY THE CONTROLLING ROD BANK

Rod No.	Rod Movement	Power Variation	
		Average Amplitude (%)	Average Period (sec)
1	UL to LL	1.7	5
2	UL to LL	0	0
3	UL to LL	1.7	6
4	UL to LL	1.4	31
5	UL to LL	1.6	10
6	UL to LL	1.4	21
7	16" to LL	1.5	9
8	UL to LL	1.5	8
9	18.7" to LL	1.7	5
10	UL to LL	1.5	7
11	UL to LL	1.6	12
12	LL to UL	0	0
13	UL to LL	1.2	17
14	20" to LL	1.4	32
15	UL to LL	1.5	7
16	LL to UL	0	0

compensated by a three rod bank. The second series, performed to supplement and confirm the first series, consisted of single rod movements compensated by a two rod set. Two rods rather than three were used because at the time this series was performed, there was no power variation unless Rod 14 was withdrawn. As shown in Figure 3.2-3, rod movements which caused flux depressions in the vicinity of Rod 14 caused the power variation to stop. Moreover, during periods of no power variation, rod movements which caused the flux to increase in the SW quadrant (thus, around Rod 14) caused the power variation to start. It was these data which led to the inspection of the removable core components in the vicinity of Rod 14 and the removal of the ACRH experiment in position J10[a].

[a]Even though the data did not indicate J8 was a likely location of the driving force, the ORNL capsules in position J8 SW and SE were also removed because of their unusual design and their nearness to the SW quadrant.

The paired rod tests mentioned earlier did not help identify the specific location of the driving force. They did, however, support the indications of the single rod tests in that increases in flux around Rod 14 caused the power variation amplitude to increase and flux depression around Rod 14 caused the amplitude to decrease.

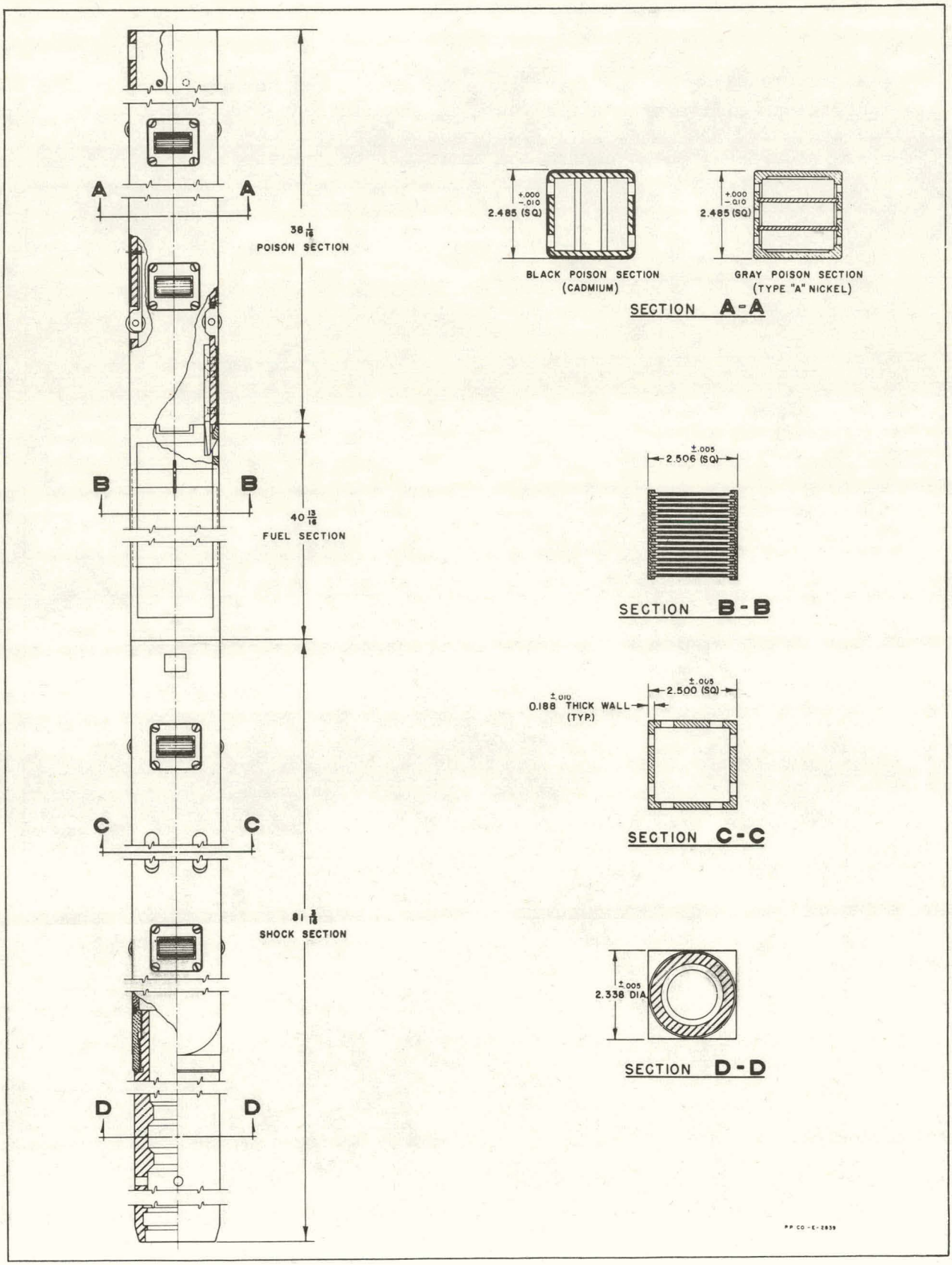

Figure 3.2-1. **ETR control rod assembly.**

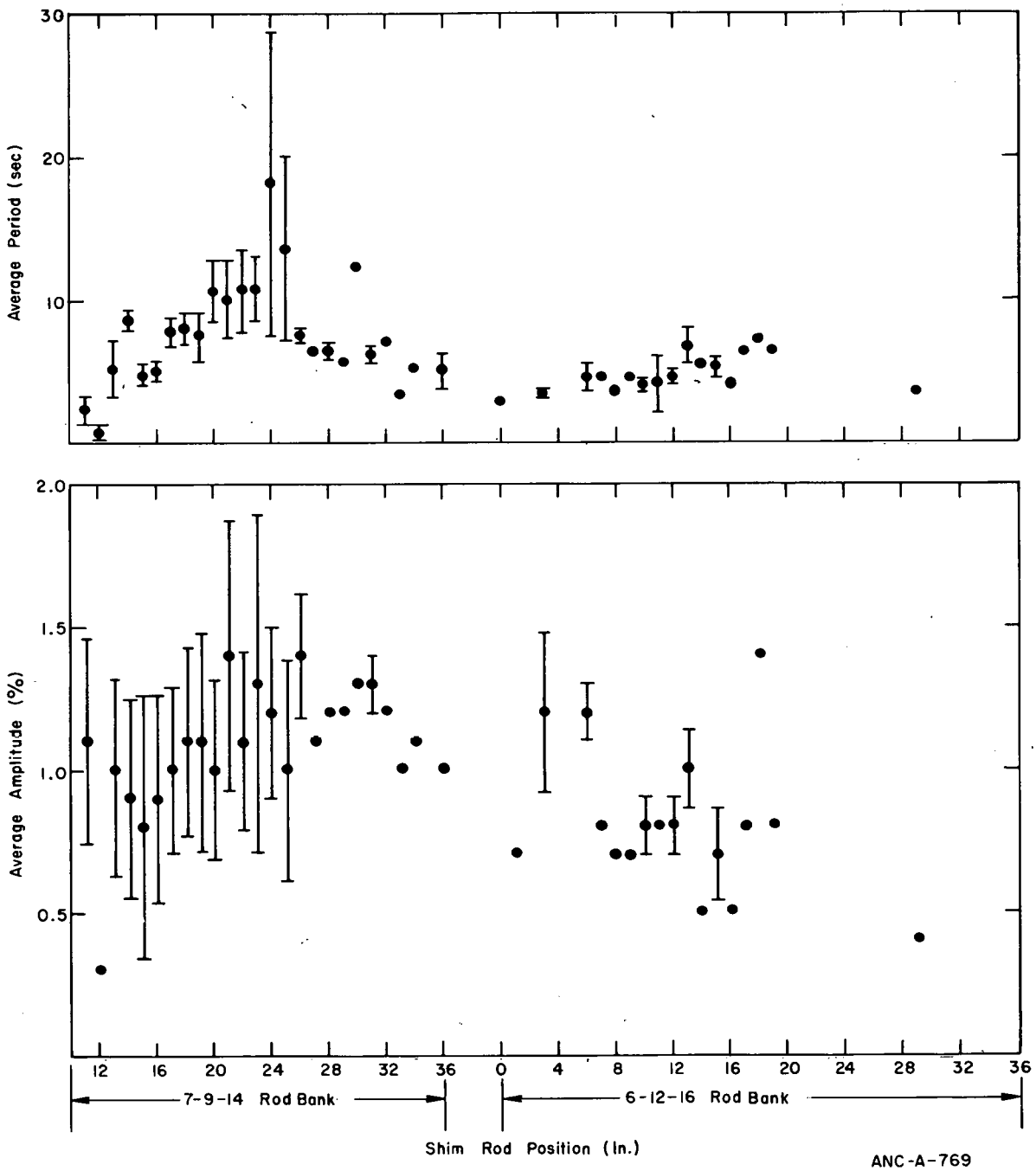

Figure 3.2-2. Effects of normal rod movement on the ETR power variation.

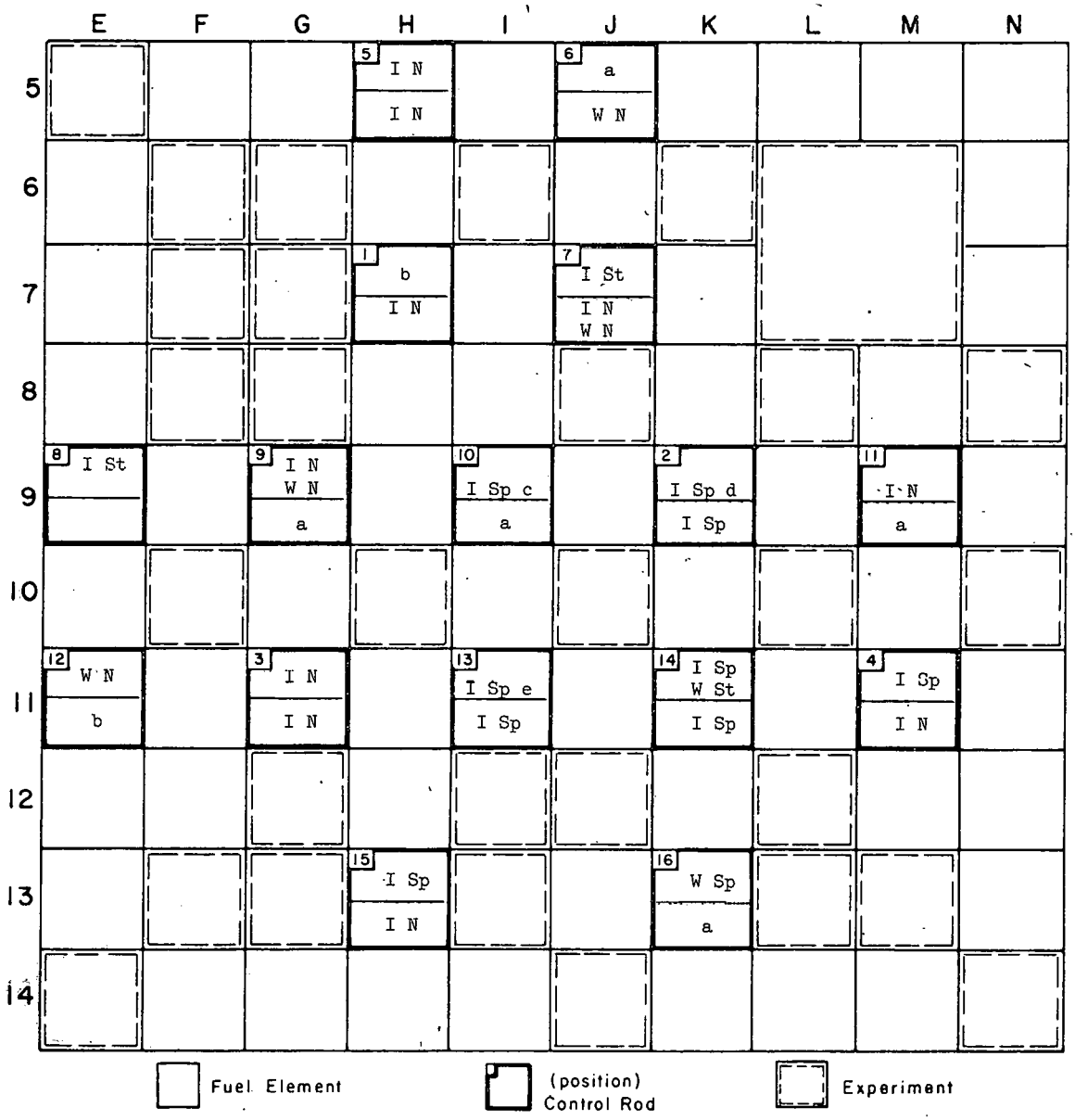

Figure 3.2-3. Results of rod effects tests on ETR power variation. Data in top half of each rod square are results of rod movement when rod bank 7-9-14 was balanced and used to compensate for rod movement. Data in the bottom half are results obtained when Rod 14 was held at UL and Rods 7 and 9 were balanced and used to compensate. Exceptions to the foregoing occurred when 7, 9, or 14 were being moved for the test. The legend is as follows:

W - Rod withdrawn for test
I - Rod inserted for test
St - Rod movement caused power variation to start
Sp - Rod movement caused power variation to stop
N - Negligible effect compared to randomness of data

a - Not Tested
b - Test results anomalous
c - PV stopped when rod reached 21"
d - PV stopped when rod reached 32"
e - PV stopped when rod reached 24"

3.3 Mechanical Movement

3.3.1 Flow-Induced Movement. Flow induced movement of core and experiment components that can influence reactor neutronics are analyzed in the following sections. These components may be forced to vibrate by the primary coolant flow. It is first necessary to examine the means of flow excitation.

Investigations of the reactor ΔP and vessel movement with primary coolant flow indicate no predominant oscillation in the gross flow at the frequencies of the observed reactivity oscillation. Local flow oscillations from phenomena such as vortex shedding require a vortex shedder on the order of several feet in diameter to obtain periods characteristic of the observed PV. Since there are no such components in the vessel, this source is not possible. Local flow oscillations from the flow pattern entering the reactor are possible. Entering flow is directed upward in the vessel from the flow distributor, turns, and travels downward into the core. Such an arrangement is likely to produce large eddies in the shear layer between the upward flow and downward flow. Before reaching the core, however, the flow passes through a 6/1 contraction area which will eliminate all large eddies. It is therefore unlikely that gross flow variations are sufficient to cause the reactivity oscillation.

Most core components which are exposed to primary flow are fixed at their downstream end and free at their upstream end. With limited movement and natural variations in pressure distribution, such an arrangement is unstable and can oscillate over a wide range of frequencies. A high degree of linearity in the "spring constant" of the support is required to cause the type of consistent waveform often seen in the reactivity oscillation. This tends to make capsule and lead experiments (which are often free standing) more likely sources than fuel elements or other core components.

To test the hypothesis that local vibration excited by turbulence might be a cause of the oscillation a test was performed in which flow was reduced while the period and amplitude of the variations were monitored.

Test conditions were: Reactor Power, 70 MW; Reactor Inlet Temperature 106°F.

Time (Hours)	Flow (% of Normal)	Variation Amplitude (Peak to Peak)	Variation Period (Sec.)
1800	100	1.7	3 - 5
2320	100	1.8	3
2349	70	1.7	2.5 - 3.5
0105	70	1.2	4 - 6
0250	70	1.1	2 - 6
0355	40	1.4	2 - 3

These data show the variability characteristic of the power variation and no flow dependence down to 40% of full flow (15% of full pressure drop). This suggests strongly that local self-excited oscillation of a mechanical part is not the source of the variation. There exists the possibility that a turbulence-excited mechanical oscillator could have a threshold below 40% of full flow. The variation in frequency exhibited by the oscillation would require a variably damped oscillator or a nonlinear oscillator. A nonlinear oscillator should show amplitude dependence and frequency dependence on the energy of the excitation force, the flow. The $\sim$ 7/1 change in this force over the test range appears conclusively to rule out this possibility. The only flow induced oscillator which remains as a possibility is one with a natural frequency dependent upon a variable damping which, nevertheless, maintains its damped natural frequency from full flow to a flow below 40% of normal.

3.3.2 Fuel Element Movement. To allow fuel element insertion and removal the ETR core was designed with a nominal 0.006 inch space between adjacent fuel assemblies and filler pieces. The assembly is located at the bottom by a tapered section on the lower end box which fits into a tapered hole in the grid plate top. Tolerances between the grid plate and the lower end of the lower end box permit 0.01 inch movement. This allows 0.040 inch movement at the top of the fuel when the fuel assembly is not restrained by other core components.

About ten years ago great difficulty was experienced in assembly and disassembly of cores, because of tightness of fuel elements. This apparently was due to mislocation of in-pile tubes. Thus, the nominal dimensions of in-pile tube fillers were reduced by 0.034 in. to permit easier core assembly and disassembly. This provided about 0.023 in. nominal space between in-pile tubes and adjacent fuel. The actual space is also affected by the location of the in-pile tube on installation, so that a relatively large horizontal movement may be permitted near in-pile tubes.

During the investigation of the power variation an attempt was made to restrict core movement by fitting oversize core filler pieces into six core positions. This test did not produce a change in reactivity variation which was attributable to the core tightening. This test does not, however, rule out fuel element movement as the source of the reactivity variation. The largest gap filled by an oversized filler piece was in position L8 (0.100 in. oversize in the north-south direction). This filler piece inserted freely, indicating a loose fit. The rod manipulation tests indicate this area is the likely reactivity source location. Therefore, fuel element movement there is a possible source.

However, two facts conclusively rule out fuel element vibration as a source: (a) the flow test described in Section 3.3.1 and the reasoning therefrom leave only one possibility--an oscillator with a distinct natural frequency which may be varied by changes in damping. Fuel

elements have mass but no spring, and cannot have a distinct frequency characteristic of a damped spring-mass system, and (b) as a very non-linear system fuel elements should exhibit flow dependence which was absent in the flow test.

3.3.3 Capsule and Lead Experiment Movement. Typical ETR capsules are inserted in X baskets in core filler pieces. The nominal clearances are 0.024 in. diametral between capsules and X baskets and 0.022 in. diametral between X baskets and core filler pieces. The X basket is fitted into the filler piece such that its movement is essentially prevented at the bottom end. The possible movement of a capsule train is, therefore, about 0.046 in. at the top plus filler piece movement and 0.024 in. at the bottom. The amount of filler piece movement is the same as for fuel elements (discussed in Section 3.3.2). Since the movement of the filler piece varies with position the total potential movement of a capsule train is approximately 0.058 in. to approximately 0.150 in. in looser portions of the core. These tolerances are typical of lead experiment and capsule movement throughout the core.

Vertical movement of lead experiments is possible if the lead tube prevents the experiment from seating fully in its position. No evidence of poor seating was found from lead experiment measurements in the course of core inventories.

Figure 3.3-1 shows reactivity changes obtained in ETRC from experiment movement. These values indicate that although experiment movement may contribute to the observed reactivity variation, the movement of a typical capsule or lead experiment is unlikely to be the sole source of the observed variation.

After inspections during the Cycle 114 shutdown two experiments were removed, along with core cleaning. The oscillation was not present during the next startup. One of these experiments, ACRH, consisted of a short stainless steel slug at the bottom of an X basket, the capsule, and two stainless steel slugs above the capsule. The second pair of experiments, ORNL 43-400 and 401, consisted of two 36-in.-long pieces supported only at top and bottom by spacer pads which maintained each end near the center of the X basket. The cessation of oscillation suggests that one of these two capsules might be the source of the oscillation, with the atypical ORNL being the more likely because of its mass and long, unsupported length. The natural frequency for mechanical oscillation of the ORNL capsule is in the > 1 Hz range and dependent upon the medium in which it is immersed. As a representative of the lowest frequency type of capsule in the reactor, this high natural frequency, relative to the observed PV period, rules out this capsule or any similar capsule as the oscillator, based on flow-induced movement. Further examination of other oscillation mechanisms for this capsule is included in the cause analysis section.

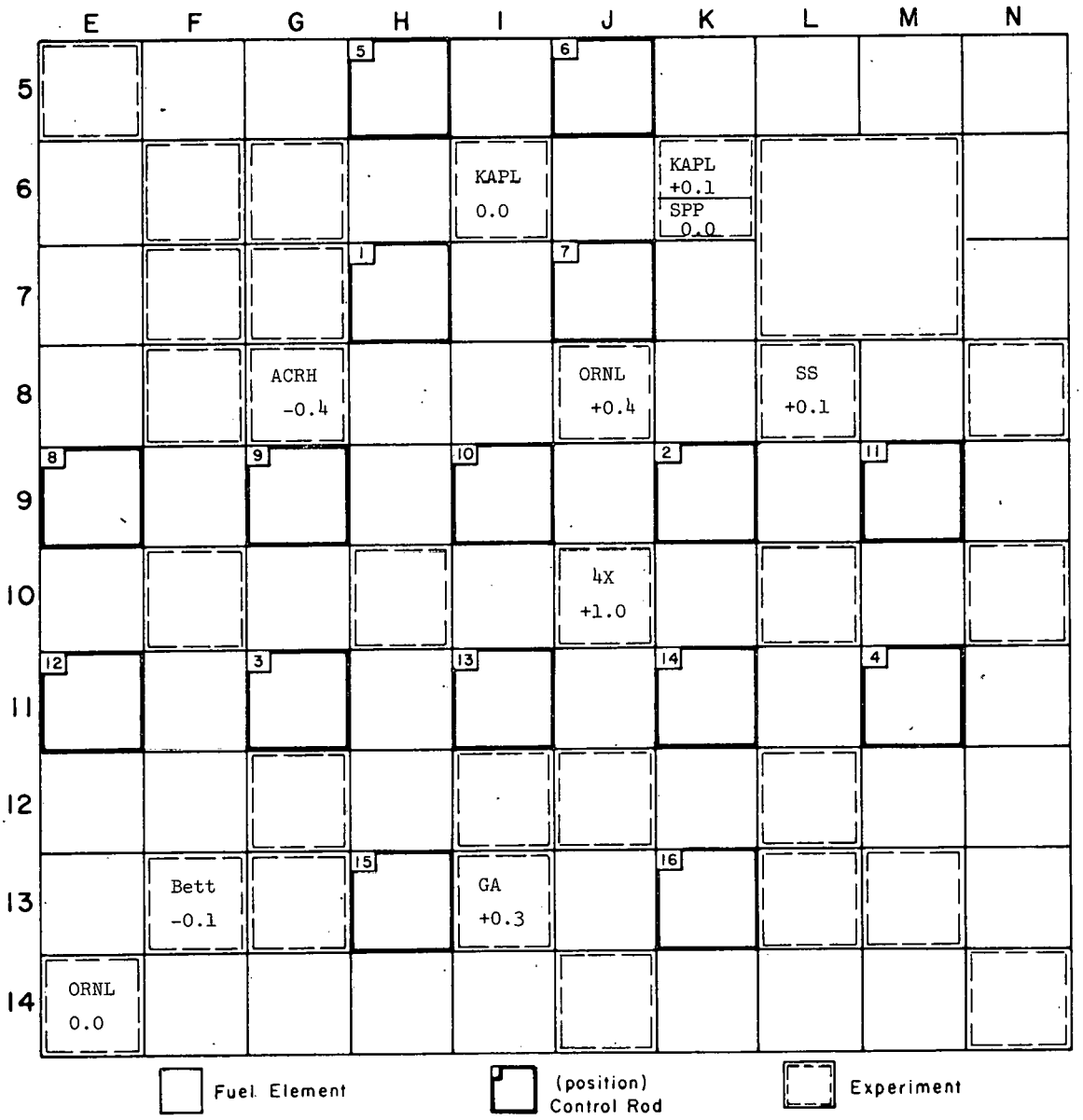

Figure 3.3-1. Maximum reactivity change (¢) observed when the indicated rod or experiment was moved laterally and/or rotated.

3.4 Gas Induced Voids

Because voids in the water within the core region can cause reactivity effects, voids are a possible source of power variations. Possible sources of voids besides boiling (see Sect. 3.6) are experiments containing pressurized gas. Three types of experiments in the ETR at the time of the power variations could cause varying reactivity effects: (a) gas filled lead experiments, (b) gas filled loop insulating annuli, and (c) gas filled leads with insulating annuli. Types (a) and (b) are pressurized to nominally 220 psi (PCS pressure is 200 psi) to preclude the admission of water should a leak develop. Types (a) and (b) contain helium. Type (c) normally contains a controllable mixture of helium and argon for the purpose of providing temperature control within the lead specimen. One of the loops was known to have a gas leak, either within or below the core region. This leak developed in the fall of 1970, several months before these power variations began. Evaluation of the gas makeup rate confirmed that the leak rate had not changed since the leak developed.

Several tests were conducted to determine if leaks from these experiments were causing the power variations. These tests were performed two and three times. They were performed twice to assure that the test was valid if the first test produced no effect. They were performed three times if there was an apparent effect from the first test. Completion of the composite test program confirmed that a gas leak was not the cause of the power variation.

The test program consisted of gas analysis of the primary system coolant, increasing the gas pressure, purging the system, and changing to a heavier gas in the M7 loop annuli. A gas analysis of the primary system coolant showed the gases to be within normal limits. The gas pressure in the loop annuli was varied between 205 and 230 psi. In order to confirm that a leak was not admitting water into the loop annuli, these systems were also purged. The absence of water was confirmed by the absence of water in the discharge. All lead pressures were increased from 220 to 250 psi, either with the common Experiment Lead Pressurizing System or the binary gas system. In order to more positively assure that the M7 annuli leak was not causing the power variation, helium was replaced with nitrogen. Nitrogen having a molecular weight seven times as heavy as helium should have reduced the leak rate to 40% of the helium rate.

3.5 Loops

It was postulated early in the diagnostic program that occurrences in the in-core sections of loops within the beryllium reflector were a possible source of the power variation. The reactivity coupling between loops outside the reflector and the core is too small for those loops to be the cause of the power variation. Mechanisms for causing power variations are as follows: (a) out-of-pile temperature variations, (b) out-of-pile induced flow variations, and (c) movement of loop in-core components through a flux gradient. Items (a) and (b) can cause power variations by coupling through the in-core temperature coefficient of reactivity. Out-of-pile temperature variation could result from heater and temperature control subsystem malfunctions. Flow variations could be caused by malfunctioning valves or intermittent and partial flow blockage anywhere in the loop. Flow variations would cause variations in test cooling rates, resulting in in-core and outlet temperature variations. Flow variations also could conceivably cause in-core component movement which would cause outlet temperature variations if the movement affected test cooling. Loop core inlet and outlet temperatures were simultaneously recorded with power level (neutron) signals. Where possible these signals were conditioned and recorded with special instrumentation that allowed any desired amplification. Using experimental data, an analysis was then made to determine the magnitude of the parameter variations that would be required to cause the observed power variation. The results of this analysis are shown in Table 3.5-I. Temperature and flow data are listed in units of percent because absolute values are classified. As shown in the Table, the observed (measured) temperature variations are at least a factor of ten too small to be the cause of the power variations.

TABLE 3.5-I

LOOP CORE-INLET AND OUTLET TEMPERATURE VARIATIONS REQUIRED TO CAUSE CORRESPONDING POWER VARIATION[a]

(All values are in units of percent)

	Inlet Temperature Variations			Outlet Temperature Variations		
Loop	Measured	Required	Ratio	Measured	Required	Ratio
L-12	<0.01	12	>120	0.21	24	110
M-7	0.07	5	71	0.19	10	54
F-10	<1[b]	12	>12	<1[b]	23	>23
H-10	0.15	13	86	0.17	24	140
M-13	<1[b]	17	>17	<1[b]	14	>14
N-14	<1[b]	13	>13	<1[b]	10	>10

[a]Power variations at the time of these measurements ranged between 0.5 and 1.1%.

[b]Special instrumentation not used - values are estimates obtained from standard loop instrumentation.

In order to give as much assurance as practical that the loops were not the source of the power variation several other evaluations and tests were made. Examination of power level recordings shows changes in power which are considered to be too fast to be caused by loop out-of-pile equipment (eg, recordings for 11/23/71, Fig. 2-7). The history of test specimen changes and loop modifications was reviewed. With one exception all test specimens installed or already in at the time of the power variation appearance (June 1, 1971) were subsequently exchanged with other specimens through a normal course of events. None of these had a correlatable effect on the power variation. The one exception was M-7. The M-7 test was installed during the 112A shutdown, May 1971, and had remained in place through Cycle 114B, Nov. 23, 1971. To assure the test was not experiencing movement or causing voiding it was removed during the 114C shutdown. Power variations still existed during 114C.

The special tests and measurements performed are as follows. Each loop temperature control subsystem was placed in manual operation with no correlative effect on power variations with periods less than 15 seconds. As mentioned before, on a few occasions temperature control problems caused small power variations with periods greater than 15 sec. Test specimen thermocouples and power monitors (thermocouples embedded in ^{235}U) along with reactor neutron signals were monitored for indications of boiling and specimen movement (movement could cause variations in cooling capabilities). Cross correlation analysis and magnitude evaluation of these signals indicated the observed variations were driven by the reactor. One significant aspect was that the specimen signals lagged the neutron signal by greater than one second. Although part of this lag is, no doubt, due to thermocouple response, it is great enough to indicate the test was not driving the reactor. The only remaining loop-associated effect which is a possible source of a power variation is movement of the loop in-core section of the pressure tube. It is believed that if the pressure tube were moving it would be affected by the primary system coolant flow, but changes in flow did not affect the power variation, see Section 3.3.

3.6 Boiling and Thermal Effects

Power variation (PV) data from Cycles 112 through 114C and data from the boiling source tests, flow reduction test, and the secondary coolant system upset were analyzed to determine the probability of and the character of a thermal-induced source of the PV in the ETR.

The data were analyzed to find any distinguishable dependence of the character of the power variations on reactor power level. Any dependence on reactor power level was examined for indications of boiling as a possible source. The data are shown in Figures 3.6-1 and 3.6-2.

Some variation with power could be seen in the amplitude and period, but the observed variations differed considerably at different times. The power dependence data had a large scatter, which increased with the number of points obtained at one power level. Therefore, no consistent dependence on reactor power level appeared to exist. However, the PV data did appear to increase between 0 and 80 MW and remain relatively constant above 80 MW, which is apparent from the data for the periods of the PV (Figure 3.6-2). In general the periods were smaller below 80 MW than above 80 MW.

A change in amplitude was detected toward the end of Cycle 113B when the average amplitude increased significantly from a 0.5 to 0.75% range to a 0.75 to 1.0% range. This end-of-cycle change and the observed significant differences between cycles and between parts of cycles indicate a rod position or local power effect, which suggests a possible thermally-induced power variation.

An examination of the variations and reactor plant data for the secondary system upset on July 27, 1971, determined that the secondary flow variations of about 6.4% caused a variation in reactor inlet temperature of $0.5^{\circ}F$, with a period of 1.3 minutes. Between the time of 1036 and 1046 hours, the inlet temperature variation caused a variation in reactor differential temperature and reactor power with the following characteristics:

	Reactor ΔT	Reactor Power from PV Trace
Average amplitude	$0.6^{\circ}F$ or 3.3%	3.27%
Average period	1.1 Minute	1 Minute

The normally observed PV with an amplitude of 1-2% and a period of 3-5 seconds also existed during the secondary system upset. This PV was not influenced or changed significantly during the secondary system upset. Therefore, it is concluded that secondary system flow or temperature variations or primary coolant system (PCS) temperature variations are not a source of the observed power variations.

Because the PV characteristic indicated a possible thermal mechanism, a series of boiling source tests and a flow reduction test were performed. During the boiling source tests reactor inlet pressure was raised from 200 to 225 psig, and reactor inlet coolant temperature was lowered from 110 to 85 at 80 MW reactor power. These pressure and temperature changes had no discernable effect on the PV. Another test was run on a period of 30-40 seconds. The PV amplitude displayed no significant change during six cycles run with balanced rods, but the PV period was an average of 35% greater at 220 psig than the period at 195 psig. The existence of a longer period at higher pressure suggests a mechanism of void buildup, in a confined space, with the void swept out when the void reaches some maximum volume. Increasing the pressure would increase the time for formation of the maximum void volume and, therefore, increase the PV period.

A power dependence portion of the boiling source tests and the rod effects test during Cycle 114C clearly demonstrated the existence of local power thresholds for the PV. The threshold was found to have a hysteresis characterized by an initiating power which was higher than the quenching power. The PV would quench at 58 MW and return at 68 MW, thus demonstrating a threshold between 60 and 70 MW. This hysteresis behavior is a characteristic of boiling and other thermal effects.

The thermal effects tests, therefore, demonstrated the following facts:

(1) Open channel boiling is not a potential PV source because of the relative insensitivity of the PV to power level, flow, pressure, and temperature.

(2) The data suggest that boiling within a confined space, or some equivalent thermal mechanism which is relatively insensitive to the PCS environment, may be the source of the power variation. This possibility is discussed in the Cause Analysis Section (5.0)

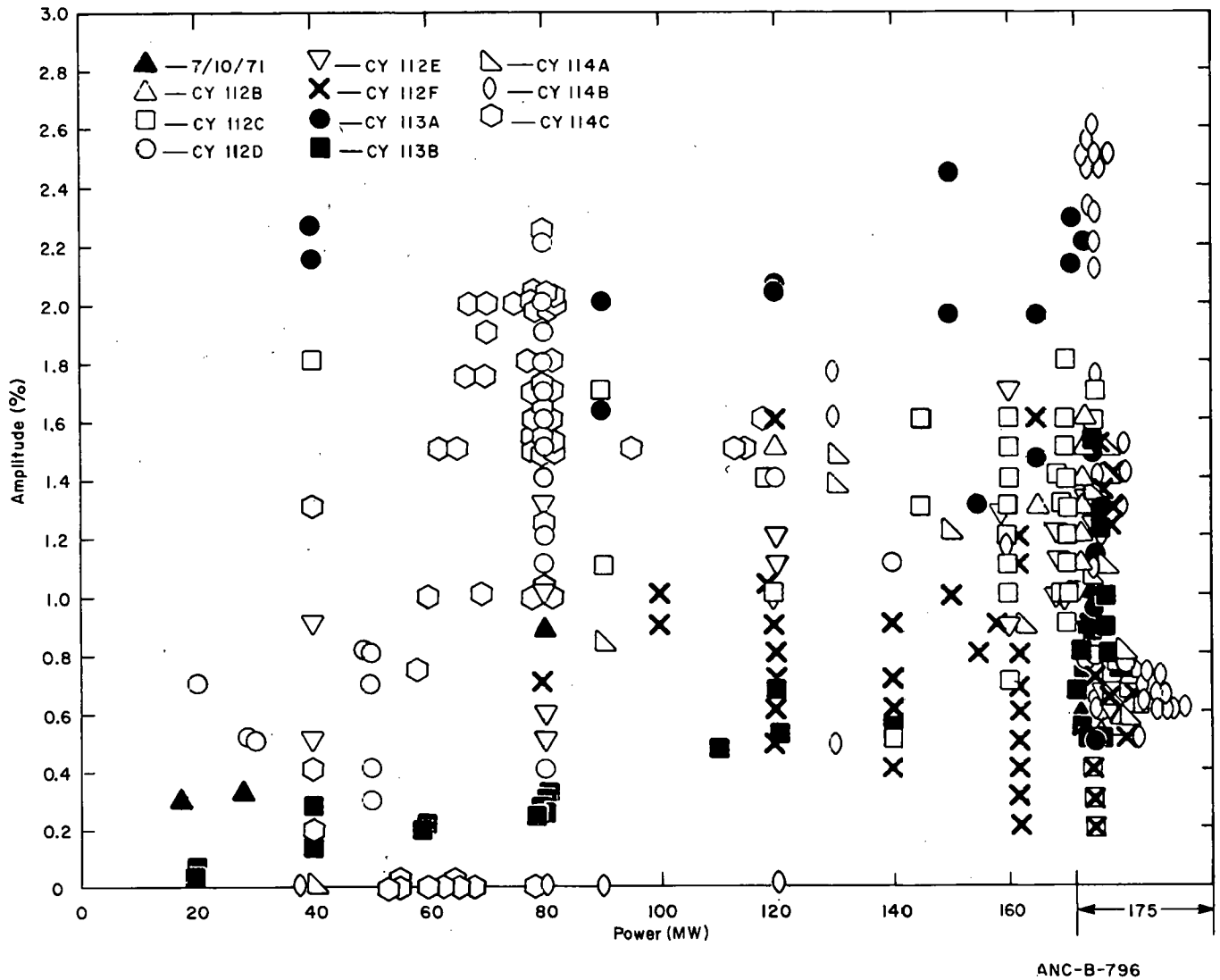

Figure 3.6-1. ETR power variation average amplitude vs reactor power.

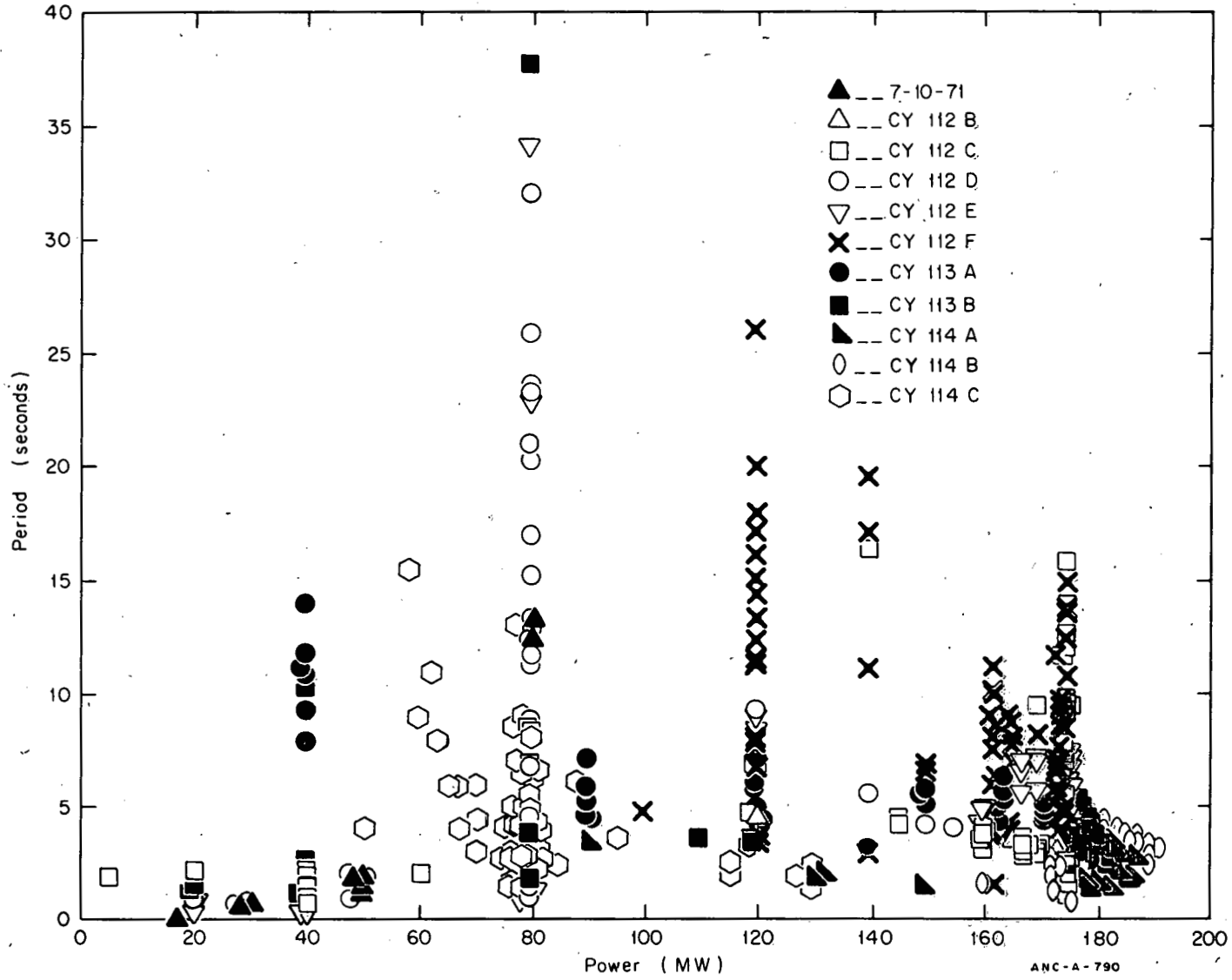

Figure 3.6-2. ETR power variation average period vs reactor power.

4. CORE COMPONENT INSPECTION

4.1 Beryllium and Lower Grid Inspection

An extensive visual inspection of the ETR grid plate and beryllium reflector walls was conducted during the 112F shutdown to determine if any failures or anomalies in these structures might be contributing to the PV.

Areas on the grid plate inspected with binoculars are shown in Figure 4.1-1. All marks viewed on the grid plate are sketched on a core arrangement drawing shown in Figure 4.1-2. Anomalies viewed were a gouge and scratch on the upper surface of the web between positions I-5 and I-6, and a nick on the south side of the I-6 hole upper surface. A deep gouge was noted on the upper surface of the web between the M-11 and N-11 positions, and a shallow gouge on the web between M-13 and N-13 positions. Cross lighting this area by different lamp positions indicated no web crack could be viewed by visual observation from the reactor top. All marks viewed appeared to be superficial and were considered inconsequential.

The beryllium reflector was also visually inspected by utilizing a mirror tool and binoculars. The beryllium core faces appeared to be in virtually new condition, very straight, and uniform at the slab interfaces. One small spall area was noted at the E-5 location, on the fifth slab where it interfaces with the fourth slab (counting down from the top). The spall area was judged to be approximately 0.75 to 1 in. long, perhaps 1.25 in. high, and shallow in depth--a very minor surface condition that may have occurred during installation of the new beryllium in 1970.

Removal of the protective cover plates on the beryllium reflector revealed particulate matter covering and probably blocking approximately 84% of the beryllium coolant holes. This particulate matter was vacuumed from the beryllium and the 0.150 in. in diameter orifice holes rodded to verify all coolant channels were open.

A second visual inspection of the ETR beryllium reflector coolant holes was conducted during Cycle 114 shutdown. The initial cursory visual examination with binoculars prior to removal of the protective cover plates indicated that particulate matter was covering approximately 25% of the visible coolant holes, causing possible blockage of coolant flow through the orifices. Removal of all cover plates indicated approximately 35% of the coolant holes had particulate matter covering the coolant hole inlet area. After photographs of the reflector top were taken the beryllium was vacuumed and then all coolant orifices were rodded with a 0.125 in. rod.

As a general observation the particulate matter was considerably less voluminous than seen previously in Cycle 112. In addition the fallout pattern on the beryllium occurred in three localized areas: (a) the northeast corner, (b) central region of the west wall, and (c) east central region of the south wall.

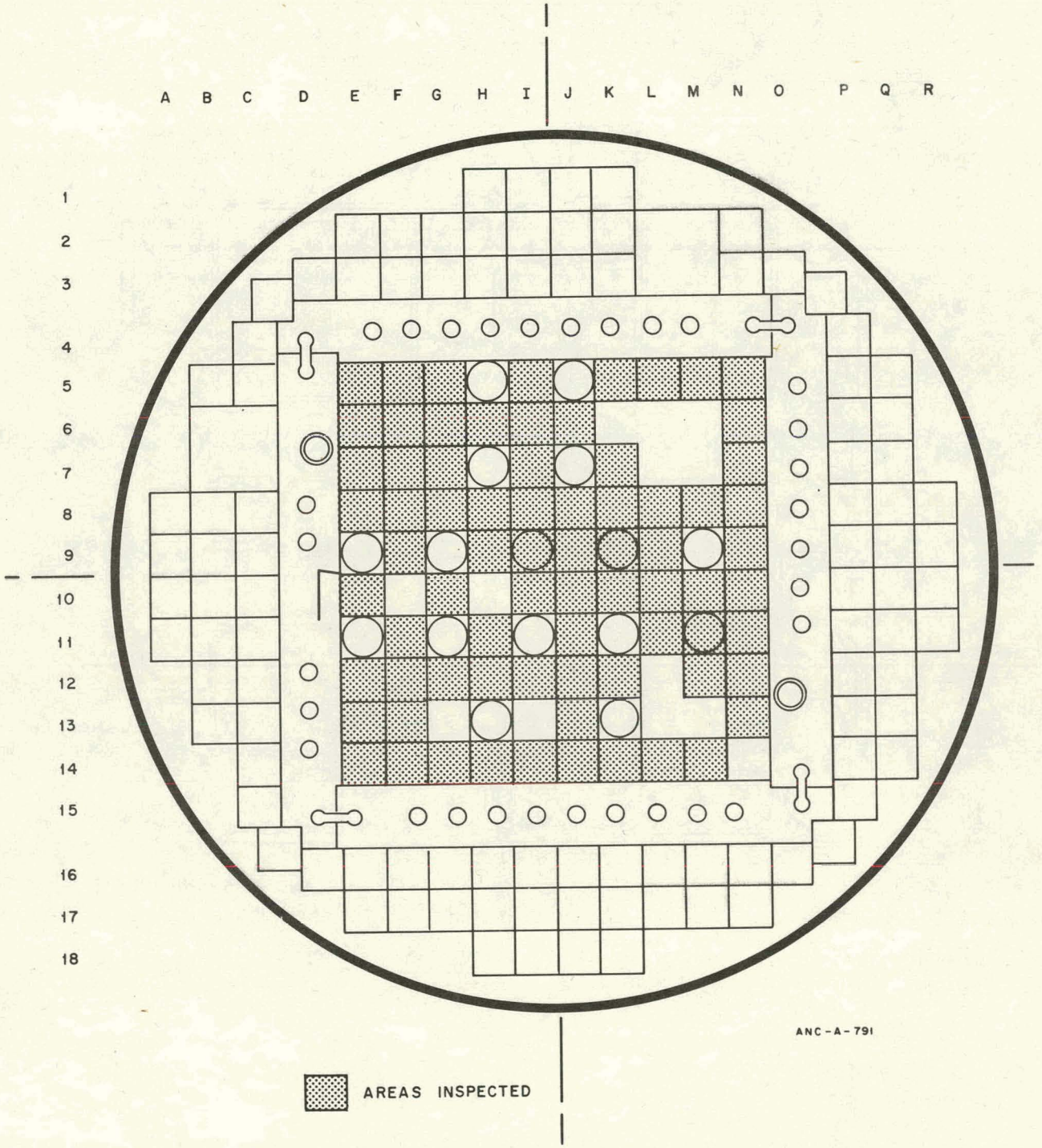

Figure 4.1-1. ETR grid plate area inspected during the 112F shutdown, 7-31-71.

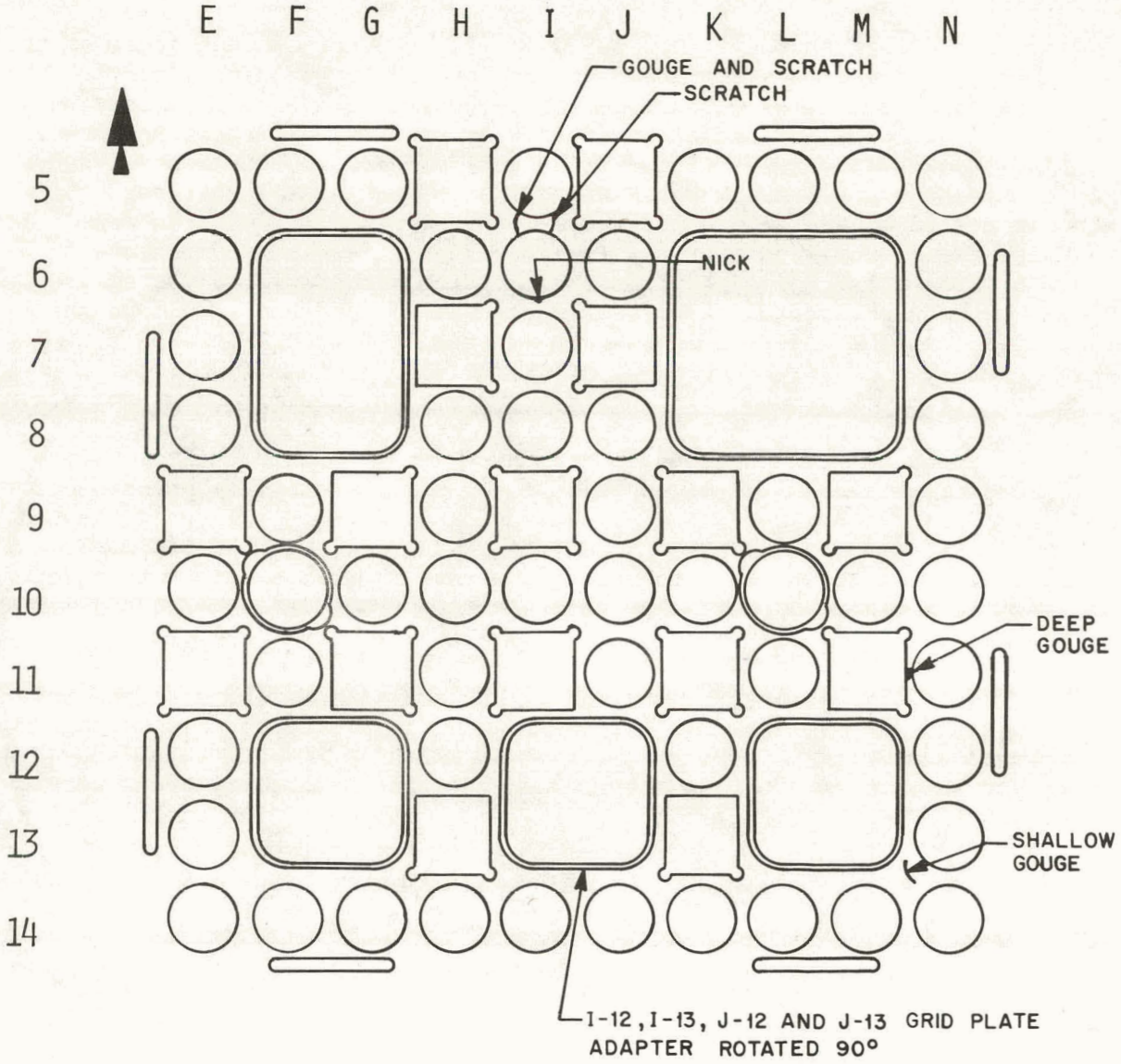

Figure 4.1-2. Damaged areas and discrepancies observed during the grid plate inspection. Shutdown 112F, 7-31-71.

ANC-A-795

4.2 Control Rods

Subsequent to the comprehensive core inspection during the Cycle 112D shutdown (July 7, 1971) the control rod components were extensively inspected on three occasions: (a) Cycle 112F shutdown (July 27, 1971), (b) Cycle 113A shutdown (August 31, 1971), and (c) Cycle 114A shutdown (October 29, 1971). General cleanliness of the rods appeared good although discoloration, rub marks, and minor scratches were observed on some of the nonfuel components. During the initial inspections some recessed or missing rollers on the poison and shock sections were found which generated a separate control rod analysis program. During the above inspections discolorations, minimal scratches and dents, and a few small pieces of debris were also found on the control rod fuel sections. Marginal components and those with recessed and missing rollers were replaced during the inspection period. These repairs produced no apparent effect on the power variations during subsequent reactor operation.

A nominal 0.57 in. gap between the poison section and guide tube is ordinarily maintained by the spring property of the rollers. Clearances between the control rod and guide tube allow for a maximum transverse movement of 0.149 in., with minimum transverse movement of 0.101 in. This assumes the roller springs are ineffective and the rod moves relative to the guide tube without tilting. If the rod moves along the diagonal from corner to opposite corner rather than side to side, the maximum movement permitted by tolerances is 0.211 in. and the minimum is 0.151 in.

Special reactivity tests involving control rod manipulations prior to the Cycle 114D shutdown (December 2, 1971) disclosed that certain rod positions of Rods No. 2, 4, 13, 14, and 16 definitely affected the power variations. During the 114D shutdown the above five rods were again disassembled and inspected. The correction of the abnormalities did not correct the PV and therefore control rod anomalies did not cause the variation.

4.3 4X Filler Piece Components and ACRH Inspections

Discovery of debris in the channels of the C4X pieces inspected during the early ETR Cycle 114A shutdown prompted additional inspection, debris sampling of removable pieces, and analysis of nonremovable core pieces. The objectives of the further investigations were as follows:

(1) Determination of possible power variations from boiling source tests and estimation of PV periods from sample operating temperatures determined by reference to the type and nature of the material or from temperatures which had become evident in the vicinity of the piece.

(2) Determination of the origin of the debris (length of time in the system and means of entry into the system).

Evaluations consisted of analysis of samples of the observed loose material for composition and structure as well as analysis of a sample of the lower slug in the ACRH experiment for metallographic characteristics, composition, and structure.

The samples of loose material were obtained from the surface of selected core and reflector pieces by scraping the surface and collecting the water and particulate matter with a special tool. Core samples were obtained during and following the Cycle 114D shutdown and reflector samples were obtained during the Cycle 114E shutdown. A summary of all the samples (with the exception of routine fuel element samples) collected from the core and reflector during Cycles 114A and 114E is shown in Table 4.3-I.

Inspection of the component surfaces during the sampling process resulted in these observations:

(1) With the exception of the 10 in. slug below the ACRH experiment, the surface film was generally loose and powdery and was easily removed. The red and black colored films appeared the least adherent to the surface.

(2) The red and black films were common to many of the stainless slugs and also appeared on some solid flow restrictors. Following operation the red color on X basket components is not uncommon. It results from high iron oxide in the aluminum oxide film, as borne out by the results in Table 4.3-I.

(3) The deep blue color on the slug below the ACRH experiment appeared to be permanent and only a small amount was retrievable from the sample for analysis. It is believed that the analyzed sample may not have accurately represented the material exhibiting the color.

The spectrochemical analysis revealed trace amounts of metals other than aluminum, particularly iron, in the samples.

TABLE 4.3-I

STATUS OF C4X SAMPLING AND INSPECTION PROGRAM

Position	Piece	History	Hole	Contents	Sampling	Results
J8	C4X-14	100-107 (in K6) 111A (in J8)	NE	SS-264	1 Sample - Film on slug	Bayerite and aluminum
J10	C4X-123	112A	NE	SS-266	2 Samples - Film on two locations on slug - Red and black color films	Bayerite and possible gibbsite in red sample. Black sample unidentified.
			SW	ACRH & 3 slugs	2 samples from lower slug. Deep blue and red color which appeared to be slug material. Samples were minute.	Bayerite and aluminum in both samples.
			SE	X-69	1 sample from X basket. Brown in color.	Bayerite with trace of iron.
				SS-69	1 sample from slug. Red and yellow.	Bayerite and aluminum possible boehmite.
J12	C4X-107	91A-109 (in I6) Canal in 110 111A (in J12)	SW	SS-263	1 sample. Slight reddish-brown in color.	Insufficient amount to process.
J14	C4X-8	91 (in J14)	NE	SS-259	1 sample. White residue with brown tinge.	Bayerite and trace of iron.
			NW	SS-71	1 sample. Red (no blue)	Bayerite and aluminum.
N12	C4X-3	105 (in G7) 114A (in N12)	NE SE NW SW	SFR SFR SFR SFR	1 sample from a hole of the C4X piece. The material was the white residue seen during inspection.	Bayerite and possible gibbsite.
					1 sample from the surface of an SFR assembly.	Bayerite and possible gibbsite.
Canal	Core filler piece	Reactor life (used to occupy core locations during shutdown)			Sample from surface.	Bayerite and possible gibbsite. Significant iron.

REFLECTOR PIECE INSPECTION

Position	Piece	Contents	Sampling	Results
R10	A Piece	Liner and SFR	A Piece - 1 sample Liner - 1 sample SFR - 1 sample	All samples - gibbsite appears to be major constituent, possible bayerite and pseudo boehmite.
R8	A Piece	Liner and SFR	A Piece - 1 sample Liner - 1 sample SFR - 1 sample	Gibbsite appears as major constituent with bayerite, pseudo boehmite, and Al metal as minor.
Q6	A Piece	Liner and SFR	Liner - 1 sample	Gibbsite is major. Significant iron.
N2	A Piece	Liner and SFR	Liner - 1 sample	Gibbsite is major. Significant iron.
I18	A Piece	Liner and SFR	A Piece - 1 sample Liner - 1 sample SFR - 1 sample	Gibbsite is major. Trace of iron and pseudo boehmite.
J18	A Piece	Liner and SFR	A Piece - 2 samples Liner - 1 sample SFR - 1 sample	(a)White area, (b) Yellow area. All samples tested gibbsite. The white area showed some Al metal. Pseudo boehmite was present.

The predominant constituent analyzed from debris in the core was bayerite (B Al_2O_3-$3H_2O$) which would indicate the film was formed at low temperature. From the literature and from reactor experience it is known that boehmite forms at temperatures considerably higher than bayerite, characteristic of the hottest fuel plates in the reactor. (The hot element in Cycle 114A exhibited boehmite on a fuel plate surface.) Boehmite was not discovered to any extent in the samples collected from the contents of the 4X pieces.

In the reflector area and on some core pieces the primary constituent appeared to be gibbsite, which is another form of the alumina tri-hydrate. Bayerite converts to gibbsite after long periods of time (>500 hr) under appropriate conditions[9].

Surface boiling in the reactor would require temperatures above the minimum boehmite formation temperature. It is concluded from this information that discovery of bayerite would preclude boiling temperatures in those locations unless the film were deposited during a low-temperature period. Appearance of gibbsite on pieces in the reflector and core area would indicate those components have experienced longer periods of operation (without handling) than components with the less stable bayerite film. The film formation history of the slug below the ACRH capsule is less evident. This capsule is discussed at length in Section 5.2.

4.4 Other Core Inspections

A comprehensive core inspection during the Cycle 112D shutdown (July 7, 1971) was initiated as part of the ETR power variation investigation. In addition to the beryllium and lower grid inspections the 9 x 9 grid adapter area was inspected; lead experiments were checked for clamping looseness, and seating; beryllium tie bars and cover plates were checked for seating and looseness; fuel elements were checked for shiny or worn spots and core tightness; and the hold-down frames were checked for excessive play. Additionally there were extensive in-place visual examinations of observable reactor vessel parts and experiment pieces. No abnormalities were observed which could account for the power variations.

4.5 Mechanism of Plugging in ETR

Plugged filler piece outlet holes which were found in the ETR were plugged by material consisting of metal and metal oxide pieces and fine metallic oxide particulate. There are two basic mechanisms by which combinations of these materials could accumulate and plug the outlet holes:

(1) Small pieces and fine particulate could adhere to the sides of the hole, slowly building up, and narrowing the hole until it completely closes. The increasing buildup must adhere well enough to not be washed off by flow through the hole.

(2) A large object or fragment of sufficient size could jam in the hole. Then the addition of smaller pieces could jam in the remaining openings. As more pieces accumulate successively smaller pieces are required to complete the plugging. This process can continue regardless of the amount of flow through the hole.

Mechanism 1 can produce only a few mils of deposit in the presence of high flow, as on TRA reactor fuel plates. There, even when the coolant water contained excessive amounts of fine oxide particulates, the deposition on fuel plates did not exceed a few mils in thickness without sluffing off. This is true even though the oxides eventually crystallize into a continuous adherent material.

If, however, a "bridge" or "dam" of fine particles forms across the hole during stagnant conditions, completely closing it, it can be maintained against a large pressure with a minimum of adhesion. Plugs found during the inspection that required large rodding forces to remove consisted only of fine particles which dispersed, once removed, suggesting that this has taken place.

Since the fine particle plugs can only be formed in essentially stagnant conditions, either during reactor shutdown or in canal storage, and only plugging by mechanism 2 can occur to any appreciable extent at normal reactor flows, it has therefore been concluded that periodic inspection and debris control will control plugging.

5. CAUSE ANALYSIS

5.1 4X Pieces with Aluminum or Stainless Steel Fillers

5.1.1 Solid Flow Restrictors. The solid flow restrictors (SFRs) are 0.25 in. inside diameter by 1.247 in. outside diameter aluminum inserts that operate in the 4X pieces without X baskets. With less than 2¼ W/g heat generation in the restrictors, the coolant can become stagnant and the heat can be removed by conduction across the annulus to the 4X pieces without reaching the saturation temperature. With more than 2¼ W/g heat generation stagnation will result in voiding the coolant annulus. If the coolant annulus remains voided the SFR will melt. However, the more likely mechanism would be complete annulus voiding, vapor expulsion, and annulus reflooding. This phenomenon would have a minimum frequency of approximately 4 cps. This frequency indicates that complete flow blockage in a 4X piece containing an SFR is not a likely source for the observed power oscillation. Longer periods are possible with partial flow blockage.

5.1.2 Stainless Steel Flow Restrictors. Stainless steel flow restrictors (SSFRs) are inserted in standard X baskets for use in 4X pieces. Coolant flow stagnation in any core position containing an SSFR will result in voiding both the annulus separating the SSFR and the X basket and the annulus between the X basket and the core piece. A stable void would result in SSFR meltdown. The more probable voiding-reflooding phenomenon would have a frequency much higher than the observed power oscillations. The frequency for one typical slug was calculated to be 31 cps. Frequency calculations indicated that flow blockage in a 4X piece containing an X basket with an SSFR is not a likely source for the observed power oscillations, because of the specific degree of flow blockage required.

5.2 ACRH Lower Slug Cause Analysis

The ACRH experiment operated in an X basket in position J10 during Cycle 114D. The X basket contained the 2 13/16 in. long ACRH experiment with 5 1/2 and 15 in. stainless slugs above the experiment and a 10 in. stainless slug below the experiment. The ACRH heat generation could be conducted across the water annulus without reaching the boiling temperatures, even under conditions of complete stagnation. The gamma heating in the stainless steel slugs cannot be removed under conditions of stagnation without causing boiling.

Inspection of the ACRH X basket components during the Cycle 114D shutdown revealed a deep blue and red color on the 10 in. slug beneath the ACRH capsule. It was believed the discoloration may have been a result of high temperatures in that region. Examination of a vertical heat generation profile in position J10 shows the peak extending into the region of the slug. If it is assumed that for some reason (debris or slug displacement) obstruction of channel flow caused temperatures in the vicinity of the slug to exceed the saturation temperature, a buildup of steam could occur causing a void which would expand until the pressure beneath the void pushed it out the top of the channel. Assuming this to happen when the void covered the complete length of the annulus, the voiding frequency would be about 31 cps under no-flow conditions. Longer periods can be postulated as a function of flow rate under conditions of partially blocked flow.

Metallurgical examinations of the stainless steel slugs were made to confirm the immediate conclusion from the coloration, namely that the colors were "temper" colors, indicating high temperatures. Confirmation would have assured that voiding had taken place in the experiment, since the range at which temper colors are produced is well above the 400°F range at which boiling initiates at ETR conditions. Examination of the grain structure indicated no high temperatures, but does not rule out operation at boiling conditions.

5.3 ORNL-43-400 and 401 Capsules

5.3.1 Experiment Description. The ORNL-43-400 and 401 experiments are noninstrumented, fueled capsules. These capsules are 1.09 in. in diameter and 36 in. long. The exterior of each capsule, which is made from a type 304 stainless steel tube 0.988 in. in diameter with an 0.060 in. wall, is surrounded by a cylindrical thermal neutron shroud of hafnium and zirconium-hafnium alloy (depending upon axial position) which has a nominal wall thickness of 0.050 in.

Each capsule contains two graphite sleeves with an 0.500 in. inner diameter, and a variable outer diameter to provide a tapered gas gap to control the irradiation temperature of the fueled test beds. The fuel test beds contain compacted pyrocarbon coated fissile and fertile particles. The fissile material is ^{235}U and the fertile material is thorium. Both materials are in the form of oxide or dicarbide ceramic microspheres forming the core of the pyrocarbon-coated particles.

The fuel beds are divided into 13 segments by graphite plugs--seven in the lower sleeve and six in the upper sleeve. Each graphite plug is separated from the fuel bed by an eighth-in. carbon felt insulator.

The maximum fissile loading is 5.0 g of ^{235}U, spread axially throughout the fuel bed length. Ten beds are approximately 2.1 in. long and three beds are approximately 1 in. long.

The assembled capsules have a spacer assembly on each end to position the experiments in X baskets. The spacer assembly has three pads located 120° apart and having an outer diameter of 1.185 in. A normal X basked has a nominal ID of 1.209 in. with 4 spacer ribs 90° apart on the inside. These ribs are to have a nominal ID of 1.154 in.

5.3.2 Investigations.

Analytical Calculations. Preliminary investigation of the experiment configuration indicated that the region where the two carbon inserts joined near the center of the experiment did not have as large a gas annulus as other positions along the experiment length. Communications with ORNL indicated their analyses had assumed each fuel bed was perfectly insulated by the carbon felt. ANC modeled the experiment using the SIMIR[10] code to determine the validity of this assumption or, if invalid, to determine heat redistributed in the carbon felt region.

ORNL data package calculations had used a low value of the gamma heating rates in the hafnium and fuel materials. ANC recalculated the heat fluxes based on correct gamma heating values in order to calculate bulk water temperature rise.

With three spacer pads on the experiments, the experiments are capable of radial movement. Also, with a nominal X basket and the pad dimensions, it is possible that the experiment could be turned such that it could be forced eccentric at the bottom end when the pad contacted the X basket rib.

Eccentricity calculations indicated that the capsules could move off-center 0.023 in., assuming all dimensions were nominal.

Velocities in the wide and narrow channels formed by moving the experiment off center were calculated assuming that the two channels were between X basket ribs. These calculations indicated velocities of 19.2 ft/sec and 31.9 ft/sec in the narrow and wide channels, respectively.

Calculations indicated limited ability to redistribute the heat from the hot stripe. The average heat flux over each segment was calculated from the SIMIR output and the bulk water temperature rise to the hot spot was calculated for each channel. The calculated temperature differentials to the hot spot were 9.24°F and 23.4°F for the narrow and wide channels, respectively.

These temperatures, with the respective heat transfer coefficients, were then used to calculate the temperature distribution for the hafnium and stainless steel in the region of the hot spot. The calculated temperatures were used for thermal bowing calculations. These calculations indicated that the thermal gradient was principally dependent upon the bulk water temperature, so the temperature gradient over the axial length was assumed linear from 0 at the top to the calculated value at the hot spot, and it was extrapolated linearly to the bottom of the capsule. The temperature was also assumed to vary linearly around the radius from the hot side to the cold side.

Based on these assumptions, the maximum unrestrained bowing was calculated to be 0.18 in., which is more than enough to force the experiment into contact with the lands on the side of the X basket.

Hot Cell Examination. Because these experiments were suspected of causing the ETR power oscillations and because the amplitude of the reactivity effect would be a function of the dimensional tolerance it was deemed necessary to check the dimensions of the experimental components, ie, the experiments and their respective X baskets.

The results of the dimensional checks indicated that the pad dimensions were within the specified tolerances and the experiments were 1.08 in. OD instead of 1.09 in.

The measurements on the X baskets indicated that the X basket, X-314, which contained ORNL-43-400 was within tolerances for the 1.209 in. ID at the points measured. However, the dimensions across the spacer ribs were large at the center of the X basket.

The X basket, X 315, which contained ORNL 43-401 was undersized in all internal dimensions.

The average measured dimensions for 0° and 90° are listed below:

	Top		Center				Bottom	
			Above Cut		Below Cut			
	Between Ribs	Across Ribs	Between Ribs	Across Ribs	Between Ribs	Across Ribs	Between Ribs	Across Ribs
X-314	1.207	1.158	1.218	1.169	1.210	1.160	1.212	1.160
X-315	1.192	1.142	1.187	1.138	1.189	1.132	1.190	1.144

Based on these measurements it is concluded that the calculations based upon nominal dimensions are applicable for ORNL-43-400 in basket X-314. However, the dimensions of the basket, X-315, which contained ORNL 43-401, restrict the movement off-center to approximately 0.005 in.

5.3.3 Transient Analysis. A transient analysis was performed using the temperature distribution model calculated for bowing. The transient was run with SIMIR and was initiated by switching the bulk water temperature and heat transfer coefficients at time greater than zero.

The results of this analysis indicate that after one second the temperatures have equalized in the SS can, and after approximately two seconds the temperature distribution is reversed from the initial steady state values.

These calculations indicate that a cycle time of 2-4 seconds would be expected under these conditions. This is approximately the frequency of the power variations.

5.3.4 Conclusions. Based on the analytical calculations and the hot cell measurements it is concluded that there is a mechanism whereby a thermally-induced movement of the ORNL 43-400 experiment could occur. The dimensions of the X basket which contained ORNL 43-401, as measured, indicate that it is not readily apparent that the ability to move eccentric is sufficient to have initiated a thermally-induced movement in this experiment.

However, these conclusions do not consider the effect of gamma flux gradients and sufficient gamma flux gradient may be available to initiate the movement.

Once the thermal bowing is initiated the mechanism exists for generating a mechanical oscillation. The bowing causes improved cooling at the hot spot that in turn results in bowing in the opposite direction. Based upon the transient calculation (Sect. 5.3.3) the frequency of this oscillation is near the frequency of the observed power variations.

6. ROD DROP EXPERIMENT AND STABILITY ANALYSIS

6.1 Summary

Rod drop experiments were performed on December 8, 1971, for the purpose of investigating the dynamic response of the reactor. The measured power reduction curve was compared to the simulated response of a reactor model. The reactor feedback model was adjusted to attain good agreement between the measured and simulated response. The stability analysis has shown that using the best estimate of the feedback models the reactor has an extremely high (theoretically infinite) margin of stability. From this analysis, the possibility that the periodic power variations observed in the reactor at full power could have been the result of reactor instability or reactor oscillation can be ruled out.

This section briefly presents the results of that work and the results of the stability analysis based on the feedback models obtained from the rod drop experiment. A detailed technical report describing the feedback models and providing more details of the stability analysis than are given in this report has been prepared[1].

The experimental procedure required dropping Rod No. 15 from its upper limit at low power ($N_L = 0.01 N_F$) and again at full power (N_F). In both cases the reactor response (power reduction) was recorded on magnetic tape simultaneously with switching signals from the clutch release and rod seat circuits. The clutch release signal provided a reference timing mark for the start of the transient and in combination with the rod seat signal a measure of the time of flight of the rod was obtained. A signal proportional to rod position was not available.

The low-power experiments were useful in confirming the effective time required for the rod reactivity insertion observed at full power. However, because of gross differences in the positions of the other rods the low-power experiments did not provide the worth of the rod or its calibration curve. Both pieces of information would have been useful in the analysis of the full-power experiment. ETR Critical Facility (ETRC) experiments also failed to provide this information because strong spatial effects were encountered due to the close proximity of the neutron detector to the ETRC core.

6.2 Analysis of Rod Drop Data

For purposes of the analysis the full-power response was considered to be divided into two parts: (a) a fast power reduction region of time duration between 200 and 300 msec, corresponding to the time during which the rod was in motion, and (b) a much more slowly varying power reduction region starting at about the time the rod was fully inserted and lasting about 25 seconds. The first power region will be called the prompt-drop region and the latter region will be called the "tail" of the power reduction curve. In this report the feedback reactivity effects are classified as prompt feedback if the response times of the feedback processes are fast enough to affect the prompt-drop region. Feedback reactivity effects which are too slow to affect the prompt-drop region are called delayed feedback reactivity effects. With these classifications in mind the analysis proceeded along the following lines:

(1) A set of reactor model equations was derived and programmed for solution by an analog computer. The computer simulation initially included only a prompt-negative feedback reactivity model, the standard six delayed neutron group, zero-power point kinetics model, a dynamic model for rod motion, and a program for simulating the "standard calibration curve" for an ETR rod. This initial model was chosen as a reasonable starting point because it is basically the model used for all reactor transient analyses up to this time. It was necessary to determine if this type of model would produce a response in agreement with the experimental response in both regions of the power reduction curve. The simulation quickly showed that the overall initial model was inadequate in both power reduction regions.

(2) Using the model described in item 1 above, the simulation studies showed that the characteristics of the tail region were affected mostly by rod worth and by the values assumed for the prompt-negative feedback coefficient. The assumed rod motion, prompt feedback time constants, and rod calibration curve shape did not affect the tail region so long as the simulated power level at the end of the prompt drop region was matched to the experimental value of the power. This match was accomplished in the simulation by adjusting the rod worth and the prompt-negative reactivity coefficients. This technique permitted studying the "tail" region dynamics separately from the prompt region dynamics. Experimentation with delayed feedback reactivity models in the simulation resulted in development of a model that produced good agreement with experimental data in the "tail" region.

(3) After a delayed feedback reactivity model was identified, the initial prompt-feedback reactivity model was modified until good agreement was obtained between the simulated response and experimental response in the prompt-drop region.

The feedback reactivity models determined from these studies consist of a prompt-negative feedback model attributed to the fast thermal response of the fuel plates and the water in the coolant channels, and a delayed-feedback model containing both positive and negative components. The delayed-positive feedback is the faster of the two delayed-feedback models and can, at least qualitatively, be attributed to the response of water in the experiments and to other themal processes such as temperature changes of the beryllium reflector and of water not flowing through the reactor core fuel region. A physical basis for the delayed-negative feedback model has not been established but this type of feedback was required to produce agreement in the shape of the power reduction curves (experimental vs simulated) in the "tail" region for times exceeding 20 seconds. It was also necessary for good agreement in the "tail" region to add a small negative reactivity ramp which is attributed to the buildup of xenon poisoning following the rod drop. Figure 6.1 illustrated how well the "nominal" feedback models (both prompt and delayed) used in the simulation agree with the experimental power reduction curve in the "tail" region. Figure 6.2 is presented to show that delayed feedback effects do affect the shape of the "tail" region. The curve labeled "N" in the figure is the same as the experimental curve. The other curve was obtained using only the prompt-negative nominal feedback. This figure shows that initially the measured power decreases more rapidly, indicating a positive-delayed feedback effect. At about 25 seconds, however, the curves cross and the experimental power is decreasing more slowly than the simulated power. This latter effect could be due to photoneutron sources incident on the fission chamber used for measuring power, or to a neutron source effect tending to level off the reactor power. The simulation studies showed that better agreement with experiment was obtained by including a delayed-negative feedback component to the feedback model than by assuming a neutron source effect.

Equally good agreement was obtained in the prompt-drop region. The nominal prompt-feedback model included a temperature dependent water temperature coefficient of reactivity based on the experimental results of Reference 11 extrapolated to full power conditions. The simulation studies also required prompt-negative feedback reactivity due to fuel plate temperature changes. The fuel temperature coefficient nominal value determined from the simulation is about 1/10 the water temperature coefficient before the rod drop (steady-state, full-power value).

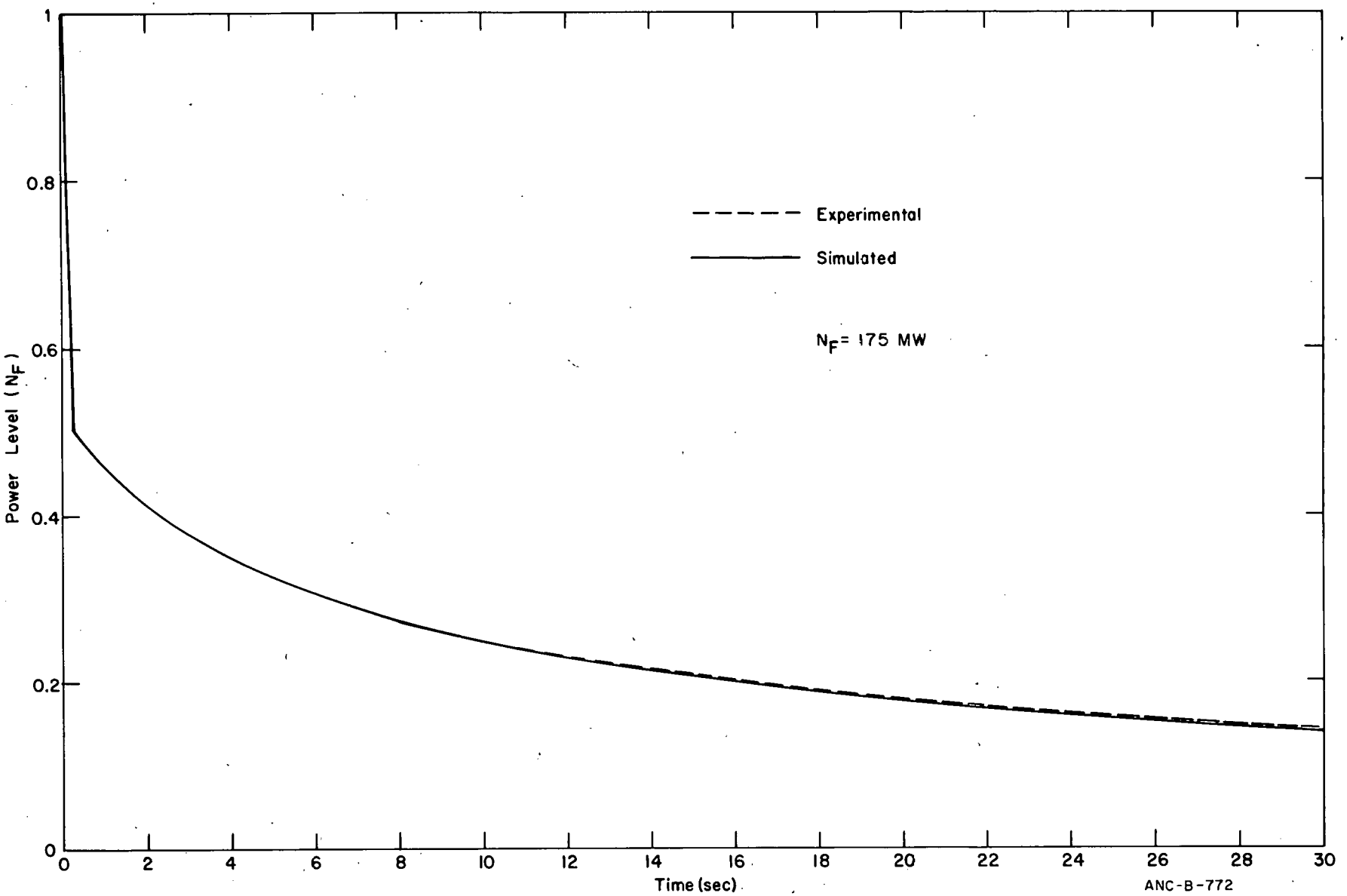

Figure 6.2-1 Super position of experimental and simulated (nominal case) power reductions "tail" region.

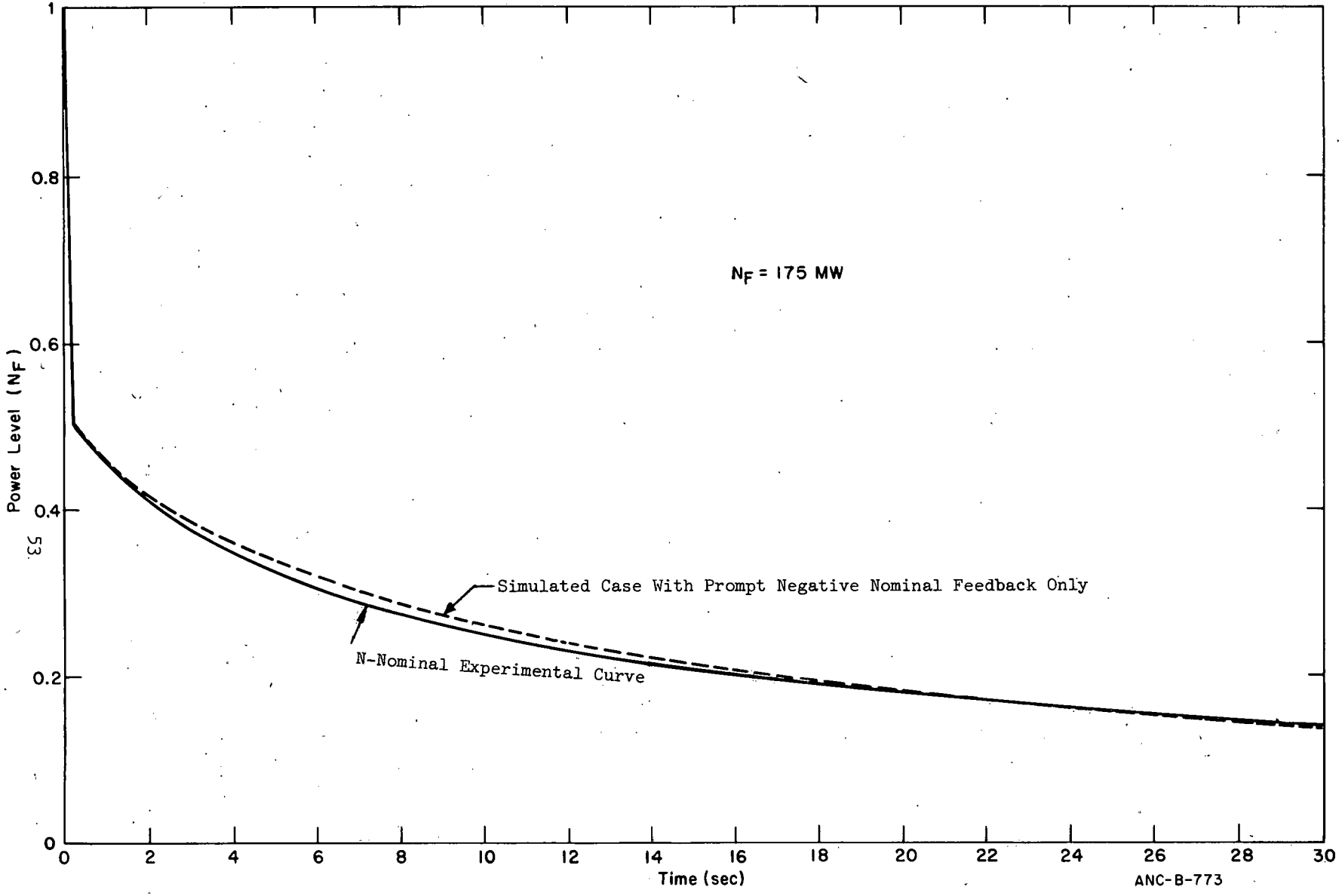

Figure 6.2-2 Effect of no delayed feedback on "tail" region of power reduction curve.

53

6.3 Discussion and Results of Stability Analysis

The feedback models described above were used for evaluating the stability of the reactor. In this analysis the zero-power reactor transfer function was combined with the feedback transfer functions to obtain the open loop and closed loop reactor transfer functions. The stability analysis was performed by application of Nyquist's stability criterion.

For the nominal feedback models (Case 1 of Table I) the stability analysis predicts an infinite gain margin and a phase margin of 110 degrees. The gain margin is defined as the net increase in system gain (product of reactor power level and feedback gain) required for the system to sustain small undamped oscillations about a steady state operating condition. Any further increase in system gain would result in divergent oscillations and the reactor would be unstable. The concept of an infinite gain margin as obtained in this analysis has meaning only for operating conditions for which the models used in the analysis are meaningful. For example, under steady power operation at less than full power with full flow and pressure and normal inlet coolant temperature the models should be valid and they could be used for predicting stability. Under steady power operation above full power, full flow, etc., the models would be valid for stability analysis up to the point where the models would be expected to change such as at the onset of boiling in the core of experiments, fuel deformation, or melting, etc. At power levels where those conditions would occur the predicted infinite gain margin may not apply and, in fact, no definite statement concerning reactor stability can be made without using a new system model for those conditions. Very large or infinite gain margins are best used as indicators of relative stability over some range of operating conditions where the models are valid. In the case of the ETR, the statement can be made that the reactor is extremely stable at conditions of full power (also at less than full power), full flow, normal inlet coolant temperature, etc. The infinite gain margin is a good indicator that the reactor is capable of sustaining undamped oscillations at full power. The statement can also be made that the reactor is stable and well damped up to the point in operating conditions where the models fail to describe the operating conditions as in the case of boiling.

The stability of the reactor was also evaluated for various other values of the feedback model parameters. In Case 2 of Table I, reducing the prompt-negative feedback gain (water and fuel temperature coefficients of reactivity) 50% results in a system with a gain margin of about 8. Further reducing this gain to zero (Case 3 of Table I) results in a gain margin of about 3.2. This latter result, although not physically meaningful, still indicates an adequate margin of stability at full power. Sustained undamped oscillations would be predicted at about three times full power if no boiling occurs.

ERRATA SHEET

ANCR 1085 - ETR Power - Variation Analysis

Please insert the attached Page 54 in place of the original Page 54 of ANCR 1085, dated August 1972.

6.3 Discussion and Results of Stability Analysis

The feedback models described above were used for evaluating the stability of the reactor. In this analysis the zero-power reactor transfer function was combined with the feedback transfer functions to obtain the open loop and closed loop reactor transfer functions. The stability analysis was performed by application of Nyquist's stability criterion.

For the nominal feedback models (Case 1 of Table I) the stability analysis predicts an infinite gain margin and a phase margin of 110 degrees. The gain margin is defined as the net increase in system gain (product of reactor power level and feedback gain) required for the system to sustain small undamped oscillations about a steady state operating condition. Any further increase in system gain would result in divergent oscillations and the reactor would be unstable. The concept of an infinite gain margin as obtained in this analysis has meaning only for operating conditions for which the models used in the analysis are meaningful. For example, under steady power operation at less than full power with full flow and pressure and normal inlet coolant temperature the models should be valid and they could be used for predicting stability. Under steady power operation above full power, full flow, etc., the models would be valid for stability analysis up to the point where the models would be expected to change such as at the onset of boiling in the core or experiments, fuel deformation, or melting, etc. At power levels where those conditions would occur the predicted infinite gain margin may not apply and, in fact, no definite statement concerning reactor stability can be made without using a new system model for those conditions. Very large or infinite gain margins are best used as indicators of relative stability over some range of operating conditions where the models are valid. In the case of the ETR, the statement can be made that the reactor is extremely stable at conditions of full power (also at less than full power), full flow, normal inlet coolant temperature, etc. The infinite gain margin is a good indicator that the reactor is not capable of sustaining undamped oscillations at full power. The statement can also be made that the reactor is stable and well damped up to the point in operating conditions where the models fail to describe the operating conditions as in the case of boiling.

The stability of the reactor was also evaluated for various other values of the feedback model parameters. In Case 2 of Table I, reducing the prompt-negative feedback gain (water and fuel temperature coefficients of reactivity) 50% results in a system with a gain margin of about 8. Further reducing this gain to zero (Case 3 of Table I) results in a gain margin of about 3.2. This latter result, although not physically meaningful, still indicates an adequate margin of stability at full power. Sustained undamped oscillations would be predicted at about three times full power if no boiling occurs.

TABLE 6.3-I

RELATIVE VALUES OF FEEDBACK MODEL PARAMETERS

	Case 1	Case 2	Case 3	Case 4	Case 5
Prompt-negative feedback gain	Nominal	½ X Nominal	0	Nominal	Nominal
Delayed-positive feedback gain	Nominal	Nominal	Nominal	2 X Nominal	2 X Nominal
Delayed-negative feedback gain	Nominal	Nominal	Nominal	Nominal	Nominal
Corresponding values of gain margin	∞	8.0	3.2	2.5	2.2

Two other cases of interest (Cases 4 and 5 of Table I) and perhaps more meaningful physically were analyzed resulting in smaller gain margins. In Case 4, the delayed-positive feedback gain was doubled. The corresponding gain margin was 2.5. This case indicates that undamped oscillation would occur at 2.5 times full power or at full power with another factor of 2.5 increase in delayed-positive feedback gain. The predicted frequency of oscillation in either event would be about 0.02 Hz. The predicted five-fold gain increase over the nominal for the delayed positive feedback model is not believed to be possible because with such a large gain, agreement between the experimental and simulated rod drop power reduction curves would not have been obtained.

In Case 5 of Table I the overall delayed feedback gain (including both positive and negative components) was doubled resulting in a gain margin of 2.2. This indicates undamped oscillations of 0.025 Hz at 2.2 times full power or at full power with this gain increased another factor of 2.2. This large a gain would also not have produced agreement with the experimental rod drop curve.

The smallest phase margin obtained from the stability studies was about 85 degrees. These large phase margins support the conclusions drawn from the gain margin information.

6.4 Discussion of Related Subjects

The delayed-positive and negative feedback models developed in this analysis do not appear to be greatly affecting reactor response or reactor stability. The physical processes giving rise to these feedbacks are not definitely known but it is reasonably certain that the delayed-positive component is produced, at least in part, by the experiments. If this component should be a strong function of the experiments and perhaps also the experiment control systems it would be of interest to confirm the delayed-feedback models should future analysis become necessary.

It appears feasible, because of the low frequencies involved, to perform "oscillator" tests with the regulating rod near full power conditions that would yield information to confirm the delayed feedback model. If an experimental and analysis technique is developed for this purpose that does not require a large amount of reactor time or greatly perturb the reactor, it could be used as a routine diagnostic test of reactor stability as experiments are added, removed, or modified.

The use of noise analysis techniques does not look as promising as the "oscillator" tests in this regard. Given a neutron detector with sufficiently high efficiency the high power, power spectral density function of the reactor could be measured. By itself, the power spectral density curve would be inconclusive. Assumptions concerning the power spectral density of the reactor noise would have to be made or possible noise sources identified (such as flow-induced noise) and their power spectral densities measured along with that of the power. Past experience with high power noise analysis in the test reactors has been quite limited and the few attempts made to date have been unsuccessful primarily because of low neutron detector efficiency, response limitations of other measuring instruments for such variables as temperature and flow, and because of the lack of a reactivity noise generator that can be used to drive the reactor.

REFERENCES

[1]S. R. Gossmann, F. R. Phelps, Evaluation of ETR Stability via Rod Drop Effects, ANCR-1084.

[2]D. R. deBoisblanc, "Test Reactor Incidents: Selected Case Histories", Incipient Failure Diagnosis for Assuring Safety and Availability of Nuclear Power Plants, CONF 671011, U. S. Atomic Energy Commission, Div. of Tech. Info., Jan. 1968, pp 370-377.

[3]F. R. Keller, Fuel Element Flow Blockage in the Engineering Test Reactor, IDO-16780, May, 1962.

[4]M. J. Graber, M. F. Marchbanks, G. W. Gibson, "Investigations of Failures in TRA Fuel Elements", Annual Progress Report on Reactor Fuels and Materials Developed for FY 1967, IN-1131, Feb. 1968, p 71.

[5]F. O. Haroldsen, "Heat Transfer Analysis of ETR Element E018D", Reactor Engineering Branch Annual Report, FY 1968, IN-1228, Feb. 1969, pp 87-96.

[6]D. R. deBoisblanc, Op Cit, p 373.

[7]K. A. Strong, "Reactivity Meter Checkout and Use", Nuclear Technology Division Annual Progress Report for Period Ending June 30, 1971, ANCR-1016, pp 183-185.

[8]S. R. Gossmann, "Reactivity Meter Theory and Design", Ibid, pp 186-196.

[9]R. S. Ondrejcin, A Mechanism for Stress Corrosion Cracking of Stainless Steel Systems, DP-1089, Dec. 1969.

[10]K. D. Richert, SIMIR--A Two Dimensional Transient and Steady State Heat Conduction Program, ANCR-1028, (to be published).

[11]D. W. Knight, "ETR Bulk Water Temperature Coefficient", Nuclear Technology Division Annual Progress Report for Period Ending June 30, 1971, ANCR-1016, pp 165-167.